Geomorphology 408 (2022) 108245

Contents lists available at ScienceDirect

Geomorphology

journal homepage: www.journals.elsevier.com/geomorphology

Seasonal response of a composite beach in relation to wave climate

Mariona Casamayor [a,*], Ignacio Alonso [a], Nieves G. Valiente [b], María José Sánchez-García [a]

[a] Instituto de Oceanografía y Cambio Global, IOCAG, Universidad de Las Palmas de Gran Canaria, Campus de Tafira, 35017 Las Palmas de Gran Canaria, Spain
[b] Met Office, Fitz Roy Road, Exeter EX1 2PB, UK

ARTICLE INFO

Keywords:
Mixed beach
Volume change
Morphodynamic parameters
Beach states

ABSTRACT

Most studies regarding coastal morphodynamic have focused on sandy beaches or beaches with a single type of sediment. Wave climate has been described as one of the main factors behind the morphological changes, although this interaction is not fully understood on composite beaches. The aim of this work is to present new insights into the seasonal variability of a composite beach called San Felipe (Gran Canaria, Spain). Statistically significant correlations were obtained between different measured morphological variables, morphodynamic parameters and the wave climate. The run-up and Iribarren number were found to be good indicators of the morphological response of a composite beach. The morphological seasonal dynamics of this composite beach enabled the definition of two morphodynamic beach states which correspond to summer and winter situations. The summer state is characterized by a profile with two different sedimentological and morphological sections: an upper part dominated by pebbles forming two berms, and a lower sandy section with a gentle slope. Spilling low-energy waves dominate and the beach follows a dissipative-intermediate pattern. The winter state is defined by a reflective-intermediate behaviour of the beach, which is narrower and steeper. Two morphological features were identified: a single storm berm and cusps along the foreshore. Plunging breakers and high-energy waves dominate during winter. Based on the results obtained in this study, a new classification of composite beaches is proposed.

1. Introduction

The vast majority of research focused on beaches deal with areas with a single dominant type of sediment (Mason and Coates, 2001). However, there are beaches with a bimodal sediment distribution (Atkinson and Esteves, 2018) ranging over three orders of magnitude from sands to gravels and boulders (Horn and Walton, 2007). Sometimes these variations in grain size occur on both a temporal and spatial scale (Holland and Elmore, 2008), and it is not clear what proportion of sand is required for a beach to be considered a mixed sand and gravel type (Mason and Coates, 2001; Horn and Walton, 2007; Holland and Elmore, 2008; Aragonés et al., 2015).

Several studies have aimed to provide a classification for gravel beaches according to their sedimentological or morphological characteristics. Bluck (1967) performed one of the first classifications of gravel beaches based on the distribution of particles according to their size and shape. Other authors also established gravel beach classifications taking into account sedimentological and morphological characteristics as well as wave conditions (e.g., Orford, 1975; Williams and Caldwell, 1988; Carter and Orford, 1993; Pye, 2001; Jennings and Shulmeister, 2002; Aragonés et al., 2015). The classification of Jennings and Shulmeister (2002) is one of the most widely used. They identified three main types of gravel beaches, with two of them having mixed sediments: mixed sand and gravel beaches and composite beaches. According to these authors, a mixed sand and gravel beach includes a constant slope with both types of sediments homogeneously distributed across the beach, whereas a composite beach could be defined as a beach with two different parts in its profile: the seaward part with a gentle slope and dominated by sand, and the landward part that is mainly gravel-dominated and steeper. Despite these classifications, there is still a lack of uniformity in the terminology used, since some authors refer indistinctly to mixed beaches, but without specifying whether they are speaking about mixed sand and gravel beaches or composite ones.

Considering mixed beaches as those environments with a bimodal sediment distribution, these systems have been the subject of many research studies which have focused on their sedimentary characteristics (Bluck, 1967; McLean and Kirk, 1969; Horn and Walton, 2007; Watt et al., 2008), sediment transport dynamics (Van Wellen et al., 2000;

* Corresponding author.
E-mail address: mariona.casamayor101@alu.ulpgc.es (M. Casamayor).

https://doi.org/10.1016/j.geomorph.2022.108245
Received 29 July 2021; Received in revised form 3 April 2022; Accepted 4 April 2022
Available online 8 April 2022

Mason and Coates, 2001; Osborne, 2005; Allan et al., 2006; Curtiss et al., 2009; Bertoni et al., 2010; Dickson et al., 2011; Grottoli et al., 2019) or morphodynamic behaviour (Kirk, 1970; Carter and Orford, 1993; Pontee et al., 2004; Ivamy and Kench, 2006; López de San et al., 2006; Pedrozo-Acuña et al., 2007; Ciavola and Castiglione, 2009; Bertoni and Sarti, 2011; Dolphin et al., 2011; Bramato et al., 2012; Roberts et al., 2013; Atkinson and Esteves, 2018; Pitman et al., 2019). However, despite the growing number of morphodynamic studies on mixed beaches in recent years (Bertoni and Sarti, 2011), the hydrodynamic processes that take place to modify the response of these beaches are not yet fully understood (Pontee et al., 2004; Ivamy and Kench, 2006). Most of these works concentrate on morphodynamic aspects of the backshore and foreshore of mixed sand and gravel beaches, whereas relatively few studies have considered the nearshore conditions of this type of beach. This may be due to both high energy conditions (Osborne, 2005; Dickson et al., 2011) and the fragility of the instrumentation (Curoy, 2012).

Despite the high complexity of mixed beaches (Buscombe and Masselink, 2006; Dickson et al., 2011), waves and tides can be considered the main drivers of its morphological response and evolution. Ivamy and Kench (2006) established the importance of tidal processes in sediment transport and the morphological behaviour of the beach under low-energy conditions. Additionally, Jennings and Shulmeister (2002) reported the importance of hydrodynamic processes on composite beaches given that the morphodynamic response depends on the tide. At high tide, the beach follows a reflective regime while at low tide conditions, due to the sandy and mild lower foreshore, the dissipative regime dominates. Wave climate and other hydrodynamic parameters that depend directly on the forcing conditions have been considered in the study of mixed beaches. Pontee et al. (2004) determined that wave climate is one of the main factors in profile changes on mixed beaches and these changes occur on a shorter timescale than in other beach types. Other research studies have found a relationship between morphological changes and some of the wave climate components such as wave height, wave period or wave energy (Powell, 1990; Pontee et al., 2004), although this correlation has not been studied in depth. Additionally, other studies demonstrate that wave run-up contributes to sediment transport of coarse-grain particles (Van Wellen et al., 2000; Pedrozo-Acuña et al., 2006) and is also responsible for the formation and remodelling of the berm (Curoy, 2012). Moreover, derived hydrodynamic parameters such as the Iribarren number also help understanding the behaviour of this type of beaches as they provide information about the hydrodynamic processes at the swash zone, which in turn generate changes in the beach face profile (Pedrozo-Acuña et al., 2008; López-Ruiz et al., 2020).

Most of these processes have been described for mixed sand and gravel beaches, leaving the beach response and evolution of composite systems poorly resolved. Hence, this research aims to provide a better understanding of the morphological response and evolution of a composite beach through the correlations with the forcing conditions and morphodynamic parameters. This study evaluates the seasonal dynamics of San Felipe Beach, a composite coastal system located in the central part of the northern coast of Gran Canaria (Spain). The response

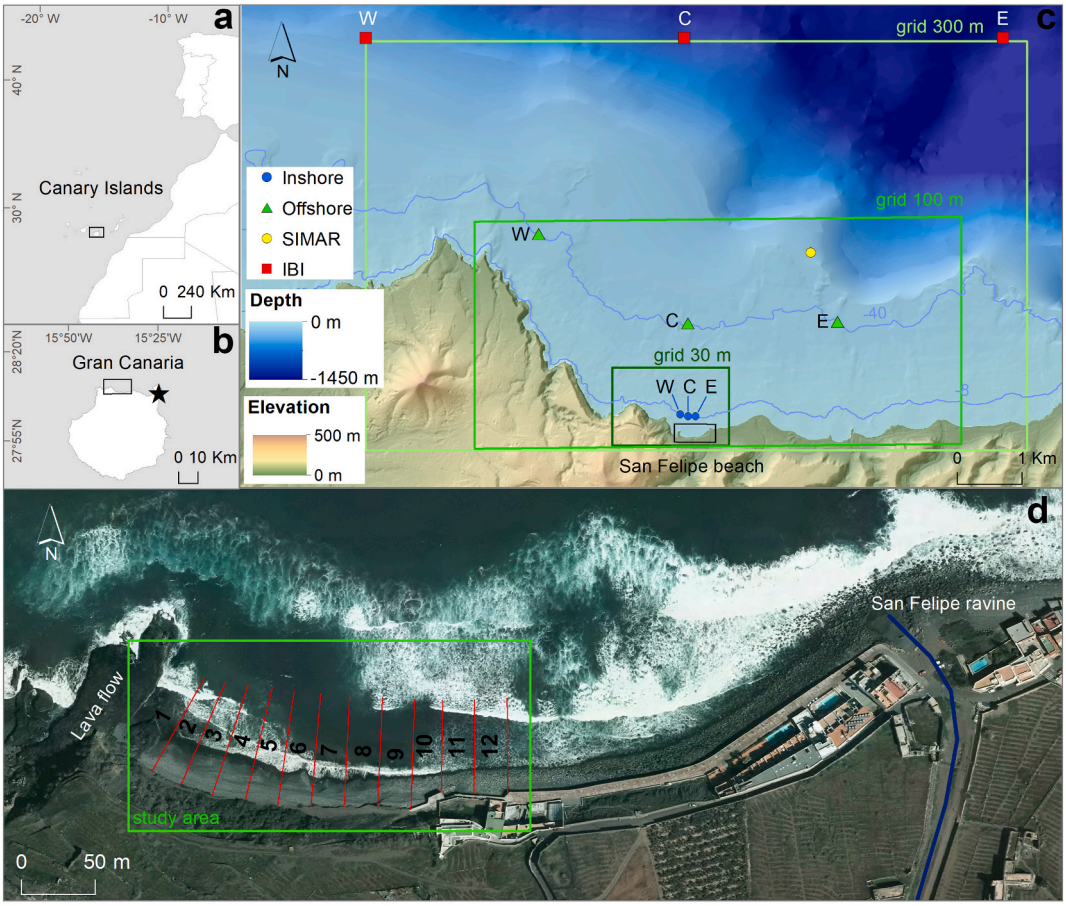

Fig. 1. a) Location map of the study area. b) Situation of the tide gauge (black star) managed by the Spanish Ports Authority in Gran Canaria Island. c) Delft3D-WAVE nested model grids (resolution of 300 × 300 m, 100 × 100 m and 30 × 30 m) and model nodes used for the extraction of bulk wave parameters. Red squares represent Iberia-Biscay-Irish (IBI) model nodes from Copernicus Marine Service used as wave input. Green triangles and blue dots indicate the offshore and the inshore nodes used in the analysis, respectively. SIMAR node 4035011 used to validate Delft3D-WAVE output data is shown as a yellow dot. d) Interpreted aerial photograph of San Felipe Beach showing the 12 profiles (red lines) used to obtain the morphological characteristics in the study area. Orthophoto source: IDECanarias, GRAFCAN S.A. (2015). (For interpretation of the references to colour in this figure legend, the reader is referred to the web version of this article.)

and evolution of San Felipe Beach using morphological observations over a period of 17 months are examined and analysed and the beach morphological changes are related to the main wave forcing parameters.

2. Regional setting

The Canary archipelago comprises a group of eight main volcanic islands and several islets located in the Atlantic Ocean (27–29° N, 13–18° W), with the easternmost islands about 100 km from the African coast.

The study area is located in a central position of the north coast of Gran Canaria island (Fig. 1), the third largest island (1560 km^2) in the archipelago. Gran Canaria is over 14 Ma and its formation can be divided into six stages. The first of these, the submarine volcanic stage, is responsible for more than 90% of the total volume of the island (Schmincke, 1982). The depth at which these volcanic materials are found means they cannot be dated. The rest of the stages are subaerial and are characterized by three magmatic stages interspersed by stages of volcanic inactivity during which erosive processes are dominant (Mangas Viñuela, 2020). The age of the volcanic materials, particularly in the case of recent volcanism, the wave incidence and the existence of giant landslides are the key factors to explain the differences in the insular shelf width (Maestro-González et al., 2005), which ranges from hundreds of meters to ten kilometres. Along the northern coast of Gran Canaria the insular shelf is very narrow, with an average width of 2.5 km (Sánchez et al., 2017). The study area is characterized by phonolitic formation of the Upper Miocene, alluvial conglomerate deposits belonging to the Roque Nublo cycle (Pliocene), and pyroclasts and basaltic lavas of the Middle Pleistocene (post-Roque Nublo cycle). The most recent materials correspond to alluvial and colluvial deposits during the Holocene (Bellido Mulas and Pineda Velasco, 2008).

All these materials became eroded and transported to the coast along the San Felipe ravine, at the mouth of which is found a fan delta. The eastern boundary of San Felipe Beach is situated at the ravine mouth, while to the west the beach is bounded by a basaltic lava flow. The southern limits of the beach are a promenade along the eastern part and colluvial deposits and debris with a steep slope in the western part.

While San Felipe Beach is approximately 450 m long, the study area only covers the western half of the beach. There were two main reasons to exclude the eastern part of the beach in this study: (*i*) sediment closer to the fan delta are mostly boulders, whereas finer materials from sand to cobble dominate in the western part, and (*ii*) the presence of the promenade blocks the normal transport of sediment to and from the backshore (Fig. 1d).

On Gran Canaria island, 30.6% of the beaches correspond to mixed beaches (Alonso et al., 2019). San Felipe is classified as a composite beach according to Jennings and Shulmeister (2002) and includes two parts with different sedimentologic and morphodynamic characteristics. The upper part of San Felipe Beach is composed of phonolitic and basaltic pebbles and cobbles throughout the year, with an average grain size (D_{50}) of 59.95 mm. The lower part has a marked seasonal behaviour due to wave climate. In winter the lower part of the beach has similar characteristics to those described for the upper part, while in summer, this part of the beach is composed of fine sand with a $D_{50} = 0.23$ mm. This thinner sediment is located in the nearshore zone forming sand bars in winter, but during summer periods when wave energy decreases, these bars migrate onshore covering the foreshore zone (Casamayor et al., 2015).

The presence of sand in the foreshore zone produces great variations both in beach width and slope. The average width is 30 m, increasing in summer (Casamayor et al., 2015). The average beach slope in the active profile is $\tan \beta = 0.1$, defined as the angle between the high and low-tide level (Bascom, 1951). The best-developed profiles are found in the central area of the beach, as the eastern profiles are limited by the promenade and those located to the west are bounded by colluvial deposits.

The Canary Islands have a semidiurnal tidal regime with mean spring and neap tide ranges of 2.8 and 0.4 m, respectively (Puertos del Estado, 2019). San Felipe is exposed to northern waves with a deep water average significant wave height (H_s) of 1.6 m and peak period (T_p) of 9.7 s. However, wave characteristics vary throughout the year, showing a clear seasonal pattern. During the summer (May–October), waves come mainly from N (49%) and NNE (33%), with a mean H_s of 1.5 m and mean T_p of 8.6 s, whereas in winter (November–April), dominant directions are from the N (36%) and NNW (31%) with a mean H_s of 1.7 m and mean T_p of 10.9 s (Puertos del Estado, 2018).

3. Data and methods

3.1. Morphological data

3.1.1. Field measurements

Eighteen topographic surveys were conducted using an electronic total station (Leica TCR 307) from October 2013 to March 2015. Both the temporal distribution and the spatial extension of each survey, especially of the subtidal zone, are highly heterogeneous since they depend fundamentally on wave and tide conditions. The temporal sequence in each survey was also strongly determined by the occurrence of storm events. The elapsed time between consecutive surveys varies from 7 days in winter when the frequency of forecast storm events was higher to 60 days in summer when wave conditions are steadier (Table 1).

Topographic surveys were conducted at low tide and were performed in spring tides to measure the maximum possible surface of the subtidal zone (Table 1).

3.1.2. Volume change and morphometric parameters

Digital elevation models (DEMs) for each survey were constructed using kriging interpolation method. These DEMs have 0.1 m spatial resolution and an average root-mean-square error (RMSE) of 0.007 m. All DEMs covered part of the subtidal zone, since topographic data were measured further seaward than the low tide mark (Table 1). The quantification of volume changes was obtained from the comparison of each survey relative to the previous one. In order to compute the sedimentary budget all DEM dimensions should be the same, therefore the most restrictive lower limit was chosen (survey of 6th February 2015).

The study area is characterized by a strong seasonal pattern, such that in summer time the pebbles and cobbles of the lower part of the beach face becomes covered by sand, whereas the upper part and the backshore are formed by pebbles and cobbles all year round (Casamayor et al., 2015). In order to obtain the volume changes in each of these two sections, it was necessary to divide the beach profile into an upper and a lower part. The limit between these two subsystems must be fixed to obtain the volume variability over time (Fig. 2). This limit between the upper and lower parts was established by comparison of summer and winter DEMs where the sedimentary budget was equal to zero, separating the upper from the lower parts of the beach where one of them shows erosion.

Three different time intervals were considered to compute the sediment budget between the largest recorded erosive/accumulative events: (i) DEMs of difference between 21st October 2013 and 14th January 2014; (ii) DEMs of difference between 14th January and 26th September 2014; and DEMs of difference between 26th September 2014 and 6th February 2015.

Twelve profiles with 20 m spatial separation were extracted from the different DEMs and used to measure beach face slope, beach width and coastline orientation (Fig. 1d). The width of the beach is defined as the distance between the head of each profile and the mean sea level (MSL) at Las Palmas Port. The beach face slope ($\tan \beta$) was also calculated considering the distance between the crest of the storm berm and the mean low water spring (MLWS = −1.14 m), and the elevation difference between both points (Fig. 2). The coastline orientation was obtained

Table 1
Survey characteristics and mean wave climate data between consecutive surveys. Survey characteristics include the date when the survey was conducted, days interval between surveys, the elevation of the most seaward measured point in the subtidal zone (minimum elevation measured) and the low tide height on the survey day (low tide height). Wave climate descriptors include mean significant wave height (H_s), mean peak period (T_p) and mean wave direction (Dir) for each interval computed in the central (C) offshore node (refer to Fig. 1c).

Id interval	Dates	Interval (days)	Minimum elevation measured (m)	Low tide height (m)	Hs (m)	Tp (s)	Dir (°)
–	Oct 21, 2013	–	−1.53	−0.89	–	–	–
1	Oct 30, 2013	9	−1.20	−0.58	1.4	12.7	353.9
2	Dec 05, 2013	36	−2.14	−1.04	1.6	11.2	9.9
3	Dec 19, 2013	14	−1.89	−0.97	1.3	14.3	358.0
4	Jan 14, 2014	26	−2.05	−0.85	1.9	14.6	356.3
5	Jan 21, 2014	7	−1.91	−0.84	2.2	13.4	359.3
6	Jan 28, 2014	7	−1.87	−0.83	2.5	10.4	14.2
7	Feb 21, 2014	24	−2.56	−0.72	2.2	13.8	0.8
8	Mar 19, 2014	26	−2.46	−1.03	1.8	11.8	9.7
9	Apr 08, 2014	20	−1.73	−0.35	1.8	11.0	4.6
10	May14, 2014	36	−1.89	−0.97	1.4	9.9	8.8
11	Jun 17, 2014	34	−2.02	−0.91	1.5	9.1	12.9
12	Jul 28, 2014	41	−2.03	−0.89	1.3	7.5	16.5
13	Sep 26, 2014	60	−1.98	−0.89	1.2	9.3	8.3
14	Nov 11, 2014	46	−1.69	−0.64	1.4	12.3	2.4
15	Dec 19, 2014	38	−2.62	−0.85	2.1	12.6	0.6
16	Feb 06, 2015	49	−2.72	−1.01	1.7	12.5	12.2
17	Mar 22, 2015	44	−2.62	−1.17	1.9	11.2	10.2

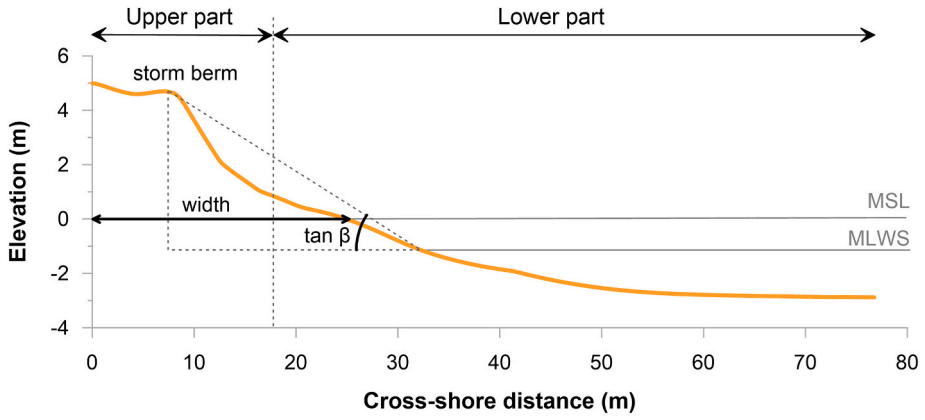

Fig. 2. Schematic representation of beach face slope (tan β) and width calculations. Two subsystems (upper and lower part of the beach) used for a detail study. MSL: mean sea level in Las Palmas Port; MLWS: mean low water spring. This beach profile corresponds to profile 6 (centre of the beach) and was obtained from the DEM of February 06, 2015.

from the angle of the contour of 0 m elevation which matches the MSL respect to north.

3.2. Wave propagation

The third-generation spectral wave model SWAN (Booij et al., 1999), packaged within Delft3D in the WAVE module, was used to transform waves from offshore to inshore. SWAN was set up using three rectangular grids with different grid cell size decreasing toward the coast (grid resolution of 300 m, 100 m and 30 m respectively). High-resolution bathymetry was created by combining bathymetric data with a summer profile. The bathymetric data were obtained using a multibeam echosounder within the framework of an echo-cartographic project run by the Spanish Government (Ministerio de Medio Ambiente, 2008) and the summer profile with the topographic data of 26th September 2014. SWAN was run with default parameters. Four dissipation mechanisms were considered: refraction, bottom friction (with JONSWAP friction coefficient of 0.067 m^2/s^2), whitecapping (Komen et al., 1984) and depth-induced breaking (with ratio of maximum individual wave height over depth equal to 0.7). In addition, non-linear wave-wave interactions were considered (TRIADS mechanism).

Time series of waves and water levels were used as model forcing. Hourly bulk parameters of wave characteristics (H_s, T_p, Dir, and directional spread) were obtained from three Iberia-Biscay-Irish (IBI) nodes (Fig. 1c) that come from a multi-year and high-resolution wave reanalysis model provided by the Copernicus Marine Service (Copernicus Marine Service, 2020). IBI nodes were linearly interpolated at intervals to the outer grid wave model boundaries. Water levels were acquired from the tide gauge the Spanish Ports Authority located in Las Palmas Port (Fig. 1b).

Due to the lack of in-situ measurements within the domain, wave model simulations were compared against SIMAR node 4035011 of the Spanish Ports Authority located in the intermediate grid (100 m resolution) (Fig. 1c).

Hydrodynamic parameters

San Felipe Beach has a concave shape. Three offshore (green triangles in Fig. 1c) and three inshore nodes (blue dots in Fig. 1c) were analysed. The central inshore node (C) was located in front of the central profiles of the study area (profiles 6–7 in Fig. 1d) at 8 m water depth. The eastern and western ones (E and W) were placed 120 m apart from the central node and at the same depth. Therefore, these three nodes cover the entire beach area. The three offshore nodes were chosen along the 40 m bathymetric contour all them aligned to the corresponding IBI node (refer to Fig. 1c).

Several wave-related parameters were obtained from SWAN in the inshore nodes: significant wave height, peak period, mean wave direc-

tion, wave length, steepness, wave energy and wave power. Wave power was computed using the Herbich (2000) equation:

$$P = \frac{1}{64\pi}\,\rho g^2 H_s^2 T_e \tag{1}$$

where ρ is water density, g is gravity and T_e is the energy period (it is assumed that $T_e \approx 0.90T_p$) (Gonçalves et al., 2014).

It is unknown if morphological changes experienced by the beach are due to specific events or to the cumulative effects of the wave climate. Therefore, following Stokes et al. (2016) and Valiente et al. (2019), the cumulative integral of wave energy (E_{cum}) and wave power (P_{cum}) were also calculated:

$$E_{cum} = \int_{t_0}^{t_n} (E - \overline{E})dt \tag{2}$$

$$P_{cum} = \int_{t_0}^{t_n} (P - \overline{P})dt \tag{3}$$

where E and P correspond to hourly values of wave energy and power, respectively, at the inshore node and $\overline{E}$ and $\overline{P}$ are the long-term mean conditions for each variable.

3.3. Morphodynamic parameters

The morphodynamic parameters relate morphological characteristics with wave climate. In general, the most widely used morphological variable is the beach slope, while in oceanographic variables it is wave height and period. However, some of the parameters use sedimentological variables instead of morphological ones.

One of the most relevant morphodynamic parameters in gravel beaches is the run-up. Several studies relate this parameter with onshore sediment transport and berm formation (Van Wellen et al., 2000; Horn and Li, 2006; Pedrozo-Acuña et al., 2006). There are different expressions for wave run-up, being those of Nielsen and Hanslow (1991) and Stockdon et al. (2006) the most used (López-Ruiz et al., 2020). This work calculated the 2% exceedance run-up using two equations. The first one was developed for a wide range of conditions on natural beaches (Stockdon et al., 2006):

$$R_s = 1.1\left(0.35 tan\beta\,(H_s L)^{1/2} + \frac{\left[H_s L\left(0.563\ tan\beta^2 + 0.004\right)\right]^{1/2}}{2}\right) \tag{4}$$

where tanβ is beach face slope, H_s is significant wave height and L is wavelength.

The second equation used comes from Poate et al. (2016):

$$R_P = 0.33 tan\beta^{0.5} T_P H_s \tag{5}$$

where tanβ is beach face slope, T_p is peak period and H_s is significant wave height. This equation is a more adequate fit for gravel beaches since it is based on data collected under energetic conditions (H_s = 1–8 m) in beaches with different grain size, ranging from gravel to pebble. Due to the importance of run-up on the morphodynamic processes on single beaches, not only two different equations have been tested, but also two different sources of wave data (from inshore and offshore nodes).

Other morphodynamic parameters such as the Iribarren number, the surf scaling parameter and Dean's parameter were calculated in order to obtain more information about the hydrodynamic processes that take place in the swash zone of mixed beaches.

The Iribarren number (ξ_b) refers to the break point (Battjes, 1974):

$$\xi_b = \frac{tan\beta}{\sqrt{(H_b/L_0)}} \tag{6}$$

where tanβ is beach face slope, H_b is breaking wave height obtained after Komar and Gaughan (1972) and L_0 is wave length in deep waters.

The surf scaling parameter (ε) was defined by Wright and Short (1984) to classify the morphodynamic state of the surf zone:

$$\varepsilon = \frac{4\pi^2 H_b}{g T_p{}^2 tan^2\beta} \tag{7}$$

where H_b is breaking wave height, g is gravity, T_p is wave peak period and tanβ is beach face slope.

Dean's parameter (Ω) was used to relate wave and sediment characteristics (Dean, 1973):

$$\Omega = \frac{H_b}{\omega_s T_p} \tag{8}$$

where H_b is breaking wave height, T_p is wave peak period and ω_s is the grain-size dependent sediment fall velocity derived from the Soulsby equation (Soulsby, 1997). Since the grain size distribution of the study beach is bimodal, ω_s was computed using two different sediment grain sizes: 0.23 mm for sand and 59.90 mm for coarse-grain particles.

3.4. Statistical analysis

In order to establish correlations between hydrodynamic and morphological parameters, the correlation coefficient and p-value were calculated to determine which of the correlations were statistically significant. These correlations were performed using both the mean and maximum values of each wave related variable. Correlations between morphodynamic parameters and morphological variables were also obtained.

4. Results

4.1. Wave model validation

Wave model Delft3D simulations were compared against SIMAR data due to the lack of in-situ measurements within the domain. SIMAR data consist of a time-series of wave and wind parameters provided by the Spanish Ports Authority. SIMAR wave data are generated using WaveWatch III numerical model, which includes refraction and shoaling effects; however, sea bottom effects can be considered negligible due to the model resolution (Puertos del Estado, 2020).

H_s and T_p are well predicted (Fig. 3), showing biases of −0.05 m and 0.36 s, respectively. The root-mean-square error (RMSE) of H_s (0.27 m) and T_p (1.92 s) show a good prediction of data. These differences between both models are mainly due to the shoaling effect which is included in Delft3D model simulations but it is not well resolved in SIMAR. Overall, the model performance is considered good at predicting wave conditions.

4.2. Wave climate

The values obtained in the three inshore nodes are very similar, although there is a small decrease in the significant wave height from west to east. Propagated wave climate data of these nodes shows a clear seasonal pattern during the study period, and they can be mainly divided into two seasons: a summer period and a winter period. Limits between these periods are not fixed, since they depend on the natural variability of the wave climate. The study period covers only one entire winter (from November 2013 to April 2014) and one summer (from May 2014 to October 2014) during the seventeen months of this study. However, as it is shown in the time-series, there is a clear seasonal pattern in wave energy (E), power (P) and wave peak period (T_p), while significant wave height (H_s) and breaking wave height (H_b) present a less pronounced seasonal behaviour (Fig. 4).

Mean wave direction is the parameter that shows the greatest differences between the three analysed inshore nodes (Fig. 5). In general,

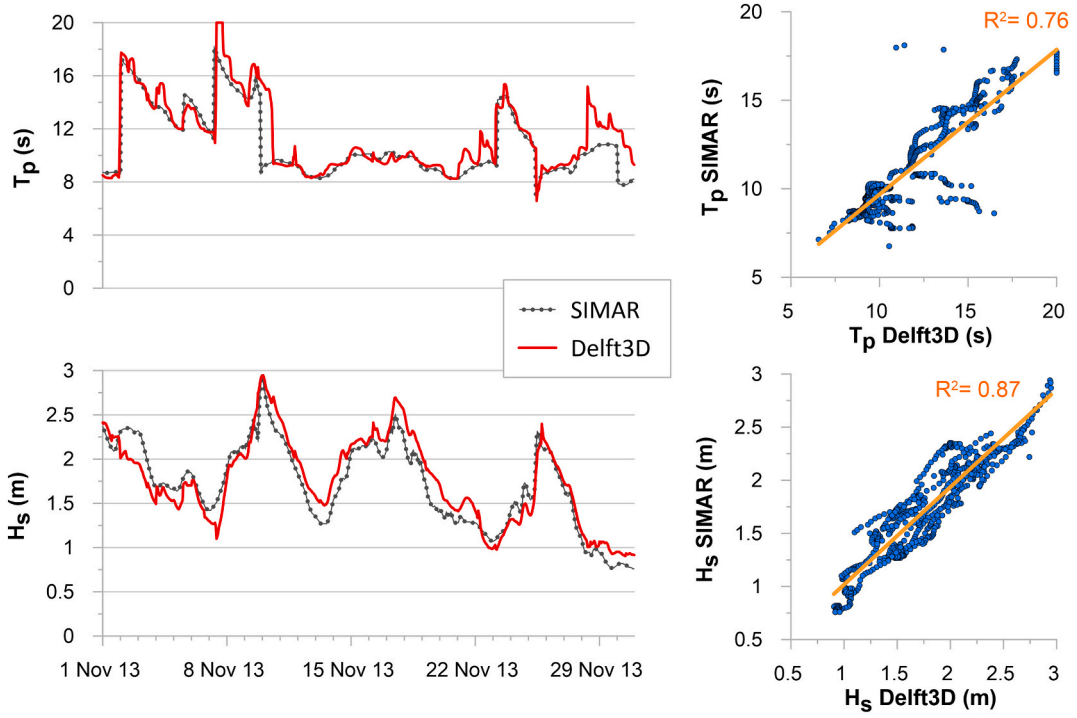

Fig. 3. Validation of the hourly wave data (significant wave height, H_s, and peak period, T_p) from 1st November to 31st November 2013. Data comparison was performed between SIMAR data and Delft3D-WAVE data corresponding to the closest node of the intermediate grid (Fig. 1c).

waves are mainly from N, although the proportion of other directions varies depend on the location of the node and the season. Regarding the only whole winter in the western node waves comes from the NNE (66%), the N (32%) and the NNW (2%) with a mean H_s of 1.6 m and a mean T_p of 12.5 s. In the central and eastern nodes most waves come from the N (92% and 99%, respectively) with a T_p very similar to the western node. However, wave height increases eastward, being $H_s = 1.7$ m for the central node and $H_s = 1.8$ m for the eastern one. In summer H_s is lower at all nodes, slightly increasing from west to east (ranging from 1.15 m to 1.22 m). T_p is also significantly lower, which indicates that during summer wind waves predominate (average T_p of 9.5 s). Wave direction also varies depending on the location of the node: in the western node the proportion of waves from the NNE increases compared to winter (66%). Likewise, in the central and eastern node N waves are dominant (77% and 98%, respectively).

In summary, despite the significant differences in H_s and T_p between both seasons, it is worthy to note that in both cases there is a slight change in H_s and direction between the different nodes, which are only 240 m apart from the western to the eastern one. The western node presents waves from the NNE while the eastern one presents wave from the N and slightly higher. Such changes in only 240 m are mostly attributed to the wave refraction induced by the dominant headland located westward of the study area (Fig. 1c).

Shown seasonal pattern is coherent with long-term evolution of H_s, since the average IBI values in winter are always higher than those in summer. Likewise, it can also be observed that the two winters of the study period correspond to the second (2.03 m) and third (1.98 m) highest average values since 1993 (Fig. 6).

4.3. Morphological response

Two morphologic features are identified in San Felipe Beach: cusps and berms. Eight of the analysed DEMs show cusps on the beach. Most of them are found in winter, except for 14th May 2014 when 5 cusps can be identified along the beach. Since these features mostly take place during winter, the horns and bays are made up of pebbles and cobbles, although some sand can also be found in the bays. The distance between horns varies from 12 to 18 m, with an average value of 15 m. The cusps are mostly located along the central part of the study area, between 0 and 1.5 m elevations in the swash zone (Fig. 7c) and their location changes even between consecutive surveys.

Berms are located in the upper part of the beach face and their elevation depends on tidal and wave conditions. In winter, the berms are found in a higher position than in summer, although two exceptions could be identified during the study period: (i) berm elevation value is higher than the average value in summer on 14th May 2014; and (ii) average elevation is low for winter on 6th February 2015. There is no clear pattern between berm length and the number of berms on the beach. Nevertheless, in winter, there is usually one single berm along the beach, which is sometimes not continuous and it can be divided into several segments. Different berms are found at different elevations in summer (Fig. 7b), with the remains of the winter berm located landwards.

Volumetric changes in San Felipe Beach show a marked seasonality. As expected, much higher volumes are observed in summer when comparing to those in winter. The most abrupt changes took place at the beginning of the two winters measured during this study. These changes correspond to the erosion of the sand in the intertidal and subtidal zones that is transported offshore ($-13{,}672$ m^3 the first winter and -8415 m^3 the second one) (Fig. 8). As the beach has no longer large volumes of sand available, the beach experiences small gains and losses of sediment during the rest of the winter period. The beach gradually accumulates sediment from May until it reaches its maximum in September. In the following months, the beach slowly erodes until a major event takes place again, eroding all the sand from the beach. When comparing the volumetric changes with the initial survey (21st October 2013), the beach after winter 2013/2014 does not completely recover and maximum volumes of sediment in the entire beach are 45% below the initial value (Fig. 8).

Regarding the upper and lower parts of the beach, it can be observed how volume changes follow opposite patterns in the two parts of the beach. During the winter months, the lower zone erodes and the sand is

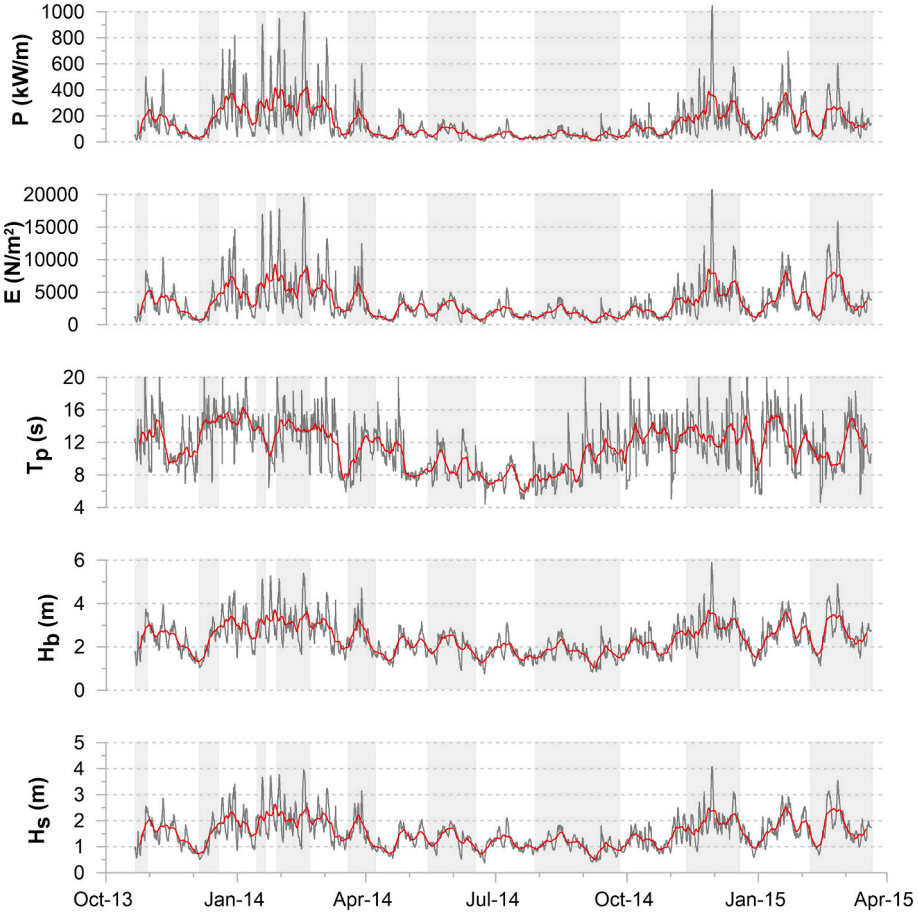

Fig. 4. Time-series of wave data corresponding to the central inshore node (C blue dot in Fig. 1c) during the study period. Red line is the running average with a window of 7 days. The gray vertical bars represent the time interval between surveys. (For interpretation of the references to colour in this figure legend, the reader is referred to the web version of this article.)

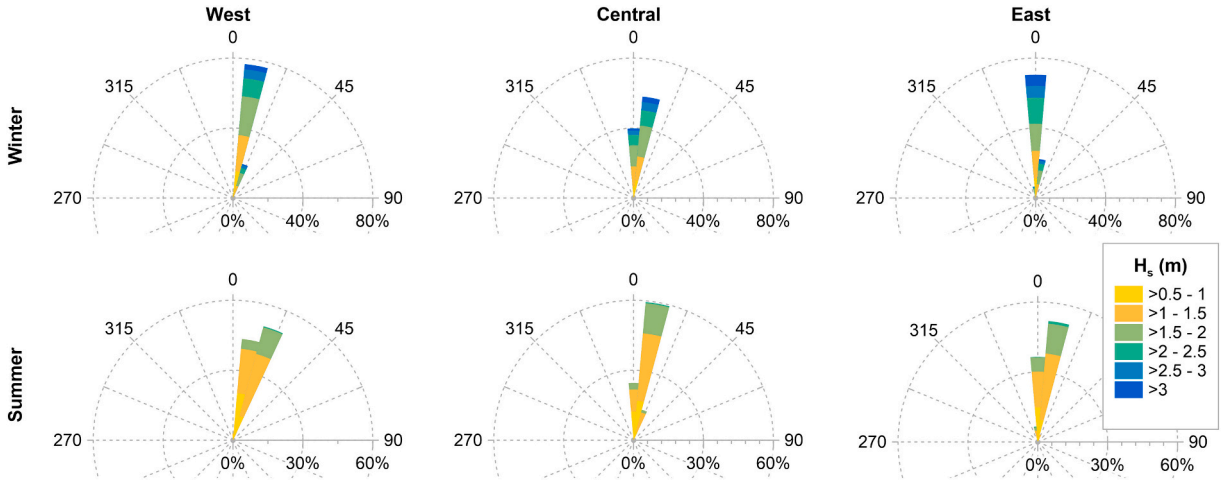

Fig. 5. Wave roses of significant wave height (H_s) at the three inshore nodes (blue dots in Fig. 1c). Upper row wave roses correspond to winter 2013/2014 (Nov 2013 to Apr 2014) and lower row wave roses represent summer 2014 (May 2014 to Oct 2014). (For interpretation of the references to colour in this figure legend, the reader is referred to the web version of this article.)

transported offshore. On the other hand, the upper zone accumulates sediment, indicating that pebbles and cobbles are transported upwards by waves. This onshore movement contributes to build up the winter berm. The opposite pattern happens in summer, with sand migrating onshore in May and reaching its maximum around September. During this period, part of the coarse-grain sediment from the upper part of the beach is steadily moved downslope, showing a net erosion along this sector. The volume changes in the upper zone are much smaller than those measured in the lower zone. Nevertheless, the correlation between the two volume evolution changes is statistically significant (p-value = 0.002 and r = −0.69) showing that when the upper zone accumulates sediment the lower area of the shoreface undergoes erosion (Fig. 8). This

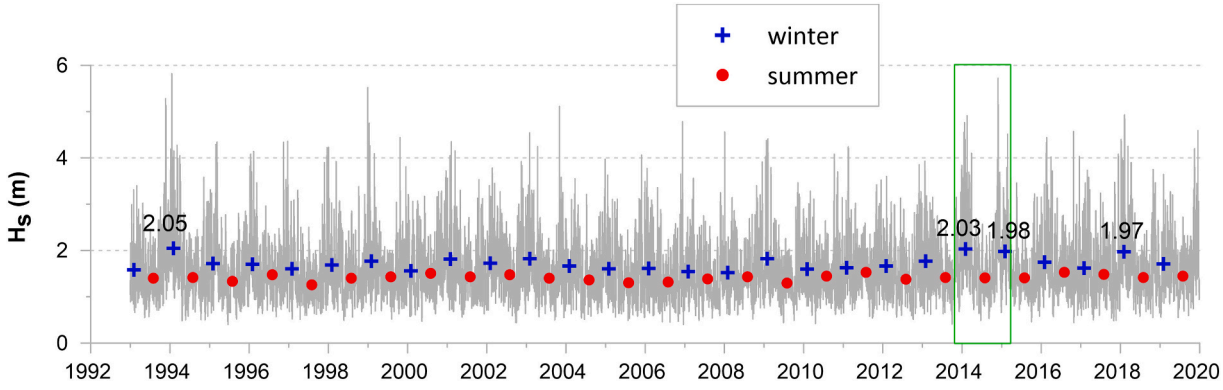

Fig. 6. Long-term series of hourly significant wave height data on the central IBI node (C red square in Fig. 1c). Green rectangle corresponds to the study period. Shown values correspond to the four largest average winters. (For interpretation of the references to colour in this figure legend, the reader is referred to the web version of this article.)

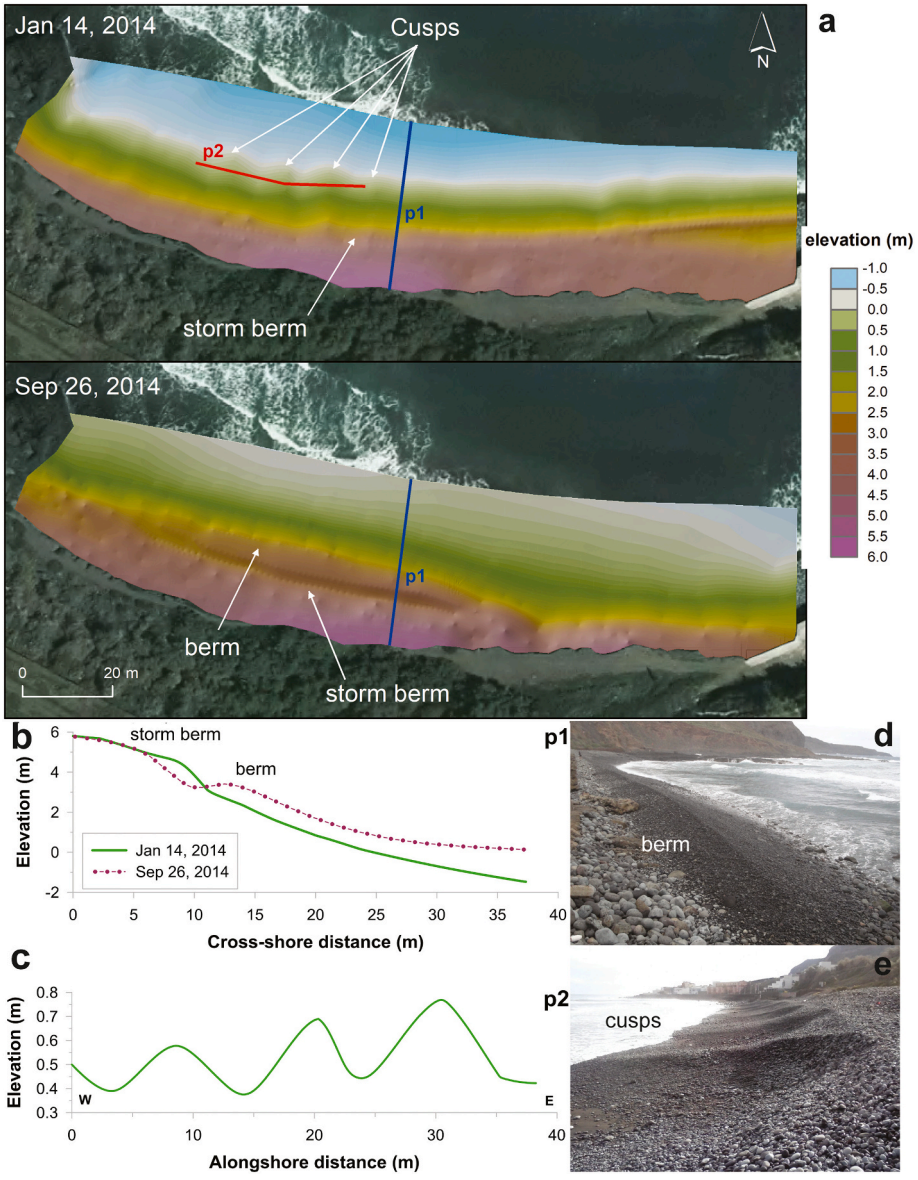

Fig. 7. a) DEMs corresponding to a winter state (14th January 2014) and a summer state (26th September 2014), showing the presence of cusps and berms. b) Profile p1 shows the storm berm built in winter and the berm. c) Alongshore transect p2 from W-E with cusps bays and horns. d) and e) Photographic examples of berms and cusps on San Felipe Beach.

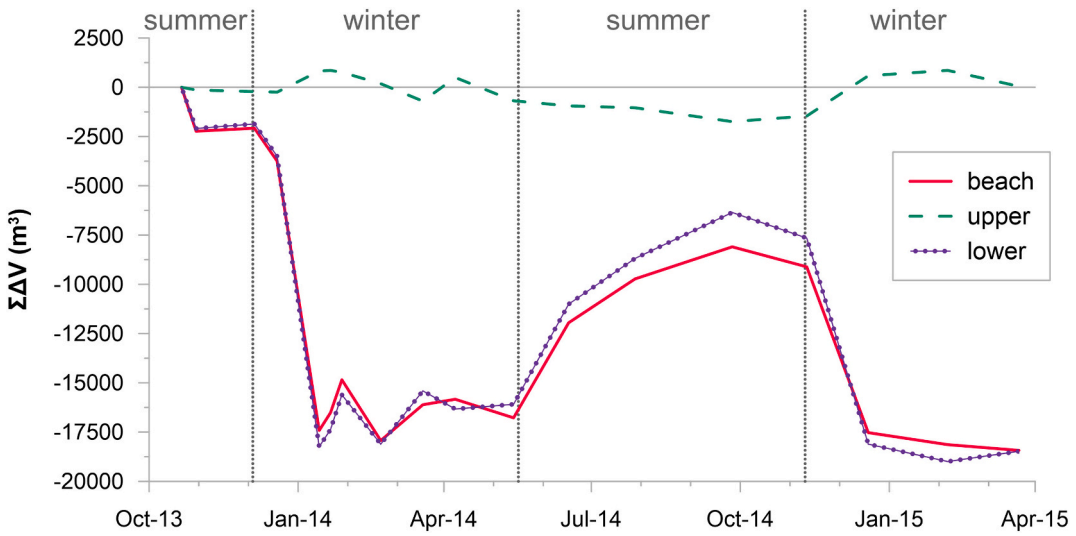

Fig. 8. Cumulative volume changes (ΣΔV) during the study period for the whole beach and the upper and lower zones.

opposite response of the two parts of the beach to similar forcing conditions highlights the need to divide the beach into two parts that are coupled: the upper zone which is fully covered by pebbles and cobbles all year round, and the lower one where sand accumulates in summer.

This division between upper and lower zones was established where the sediment budget computed from representative summer/winter DEMs was equal to zero. The three analysed time intervals previously described present a mean standard deviation of 42 m^3. Considering that the volume change between the first and the last survey is 18,429 m^3, the average standard deviation only accounts for 0.2% of the volume change. Therefore, the limit established to separate the beach into two parts was defined from the sediment budget of one the most representative DEMs for winter (6th Feb 2015) and summer (26th Sep 2014) (Fig. 9).

The rest of the morphological variables also show a strong seasonal variability (Fig. 10). The beach face slope during winter increases with an average value of $\tan\beta = 0.147$, while in summer, due to the onshore migration of the sand bar that covers the lower part of the foreshore, the slope decreases with a mean $\tan\beta = 0.072$. The width of the beach varies by almost a factor of 2 from one season to another, with the minimum value of 21.8 m recorded on 21st January 2014, and the maximum of 45.2 m on 21st October 2013. Finally, the variation in coastline orientation is small (8.61°), although it also presents a seasonal pattern: in summer the dominant direction of the coastline is WNW- ESE, while in winter it rotates to W-E.

Both the beach face width and the coastline orientation have an opposite behaviour to the beach slope: in the winter period they decrease and in summer increase. This is reflected in the statistically significant correlation (p-value < 0.01) between slope and width ($r = -0.88$), slope and coastline orientation ($r = -0.89$) and width and coastline orientation ($r = 0.84$) (Fig. 10). These morphological variables also show a good correlation with volumetric changes. Cumulative net volume of the beach has a statistically significant correlation (p-value < 0.01) with slope ($r = -0.95$), width ($r = 0.95$) and coastline orientation ($r = 0.85$). All correlations are positive except for slope, the steeper the beach is, the more erosion it experiences. Regarding the division of the beach, the correlation coefficients between the volumetric change of the lower part of the beach and the rest of the morphological parameters are very similar to those with respect to the volumetric change of the entire beach. However, the upper part of the beach only presents a weak correlation with slope ($r = 0.70$) and does not have a statistically significant correlation with the rest of the morphological variables (p-value > 0.01) (Fig. 10).

4.4. Morphodynamic behaviour

Wave data from the offshore nodes (green triangles in Fig. 1c) were used to compute several morphodynamic parameters: Run-up with two different equations (R_P and R_S), Iribarren number (ξ_b), surf scaling parameter (ε) and Dean's parameter with two different grain-size (Ω_{sand} and Ω_{pebble}). After some sensitivity analysis, it is noted that differences between the three nodes (W, C, E) are very small and can be considered insignificant.

According to the classification of beaches based on the surf scaling parameter (ε), San Felipe Beach could be reflective, intermediate or dissipative. However, this morphodynamic parameter also presents a certain seasonal pattern. The average values for the different survey periods show that the beach mostly behaves as intermediate (average ε of 10.72 for the study period). It should be noted that there are three periods in which a dissipative character dominates (intervals 1, 2 and 13, all corresponding to summer situations) and three with a reflective character (intervals 4, 5 and 16, all corresponding to winter periods) (Fig. 11).

Dean's parameter (Ω) presents two different ranges depending on whether ω_s was computed from the median sand values ($D_{50} = 0.23$ mm) or from the pebbles/cobbles mode ($D_{50} = 59.90$ mm). In both cases, the temporal evolution is the same but in a different range, since D_{50}, used to calculate the settling velocity of grains, remains constant throughout the study period. When D_{50} corresponds to pebble grain size, Dean's parameter has values between 0.07 and 0.48, all of them associated to a reflective beach. On the other hand, when D_{50} reflects the sand fraction, the variation is much greater, from 2.44 to 17.98, and the beach state changes from intermediate to dissipative, with the latter being the dominant one (Fig. 11).

4.5. Correlation between wave variables and morphodynamic parameters

The result of the analysis between the morphological, morphodynamic and hydrodynamic variables shows that there are different statistically significant correlations (p-values < 0.01). In general, the best correlations are found between morphodynamic and morphological parameters. Although some of the wave climate variables show significant correlations, their correlation is weaker (Table 2). This analysis was conducted using the three offshore and inshore nodes. The results show that correlations coefficients are very similar between the different inshore and offshore nodes, showing a maximum standard deviation of 0.012 and 0.026, respectively. For this reason, only results for the central inshore and offshore nodes are developed below.

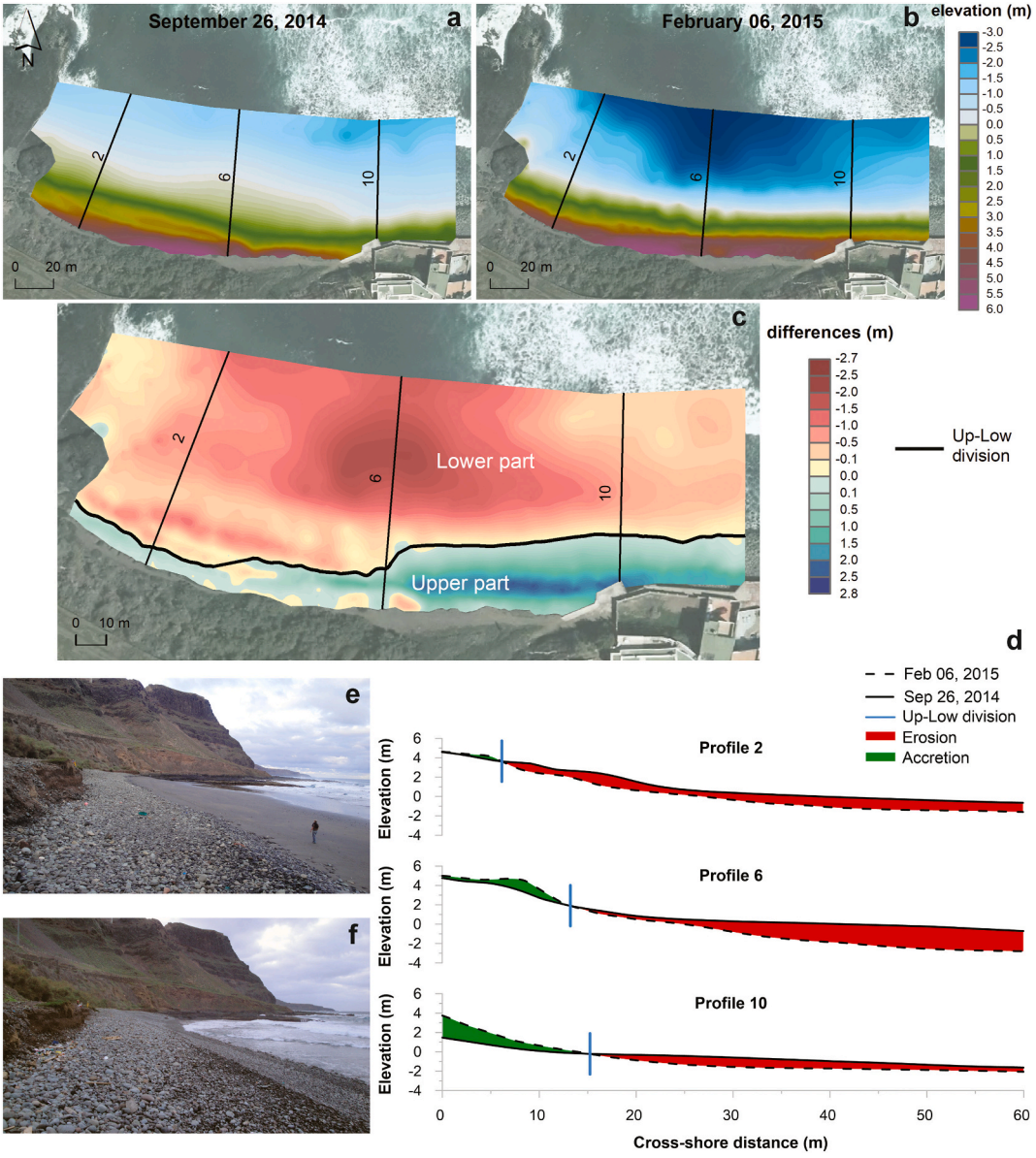

Fig. 9. a) Summer DEM (26th September 2014) with the location of three profiles (Fig. 1d). b) Winter DEM (6th February 2015). c) Sediment budget between both DEMs. d) Profile comparison between summer (26th September 2014) and winter (6th February 2015) DEMs. e) Low tide summer photograph (26th September 2014), with lots of sand in the lower foreshore. f) Winter profile at low tide with no sand in the intertidal zone (28th January 2014).

Correlations between the cumulative volumetric changes of the entire beach and the wave variables are poor, and the only statistically significant correlation is with the significant wave height (Table 2). When the wave height increases the beach erodes, while conversely, when the wave height decreases the beach accumulates sediment. However, when considering the upper and lower parts of the beach, the behaviour is different. The volumetric changes of the upper and the lower parts show opposite correlations with wave height, wave energy and wave power. In other words, when H_s, E or P increase, the upper part accumulates sediment while the lower part erodes (Table 2).

It should also be noted that E_{cum} and P_{cum} only show statistically significant correlation coefficients with volumetric changes in the upper part and beach face slope. These are quite similar to those obtained with E and P, but slightly better in the case of volumetric changes and slightly poorer for tanβ. E_{cum} also shows correlation with volumetric changes in the lower part, although it is weaker (R = -0.63).

There is a positive correlation between beach face slope and some of the wave climate variables such as wave height (both significant and breaking), wave energy and wave power. This relation is bidirectional, therefore, when any of these variables increase, the beach slope also increases and vice versa (Table 2).

Beach width does not have a statistically significant correlation with any of the wave climate variables, while the coastline orientation presents a negative correlation with most of them (Table 2). When wave height and energy are greater, the coastline angle is smaller, which indicates that the beach is more parallel to the W-E axis, whereas when the wave height and energy decreases, the coastline slightly rotates to a WNW-ESE direction.

The wave run-up correlates well with all the morphological variables. The run-up obtained following Stockdon's equation (Eq. (4)) using offshore wave data shows higher correlation values with the morphological variables, except for volumetric changes in the upper part which have a slightly better fit with the run-up obtained from Poate's equation (Eq. (5)). The R_P values are higher in winter and therefore have a better fit with the volumetric changes in the upper part of the beach that require energetic waves with high tide conditions. Both run-up

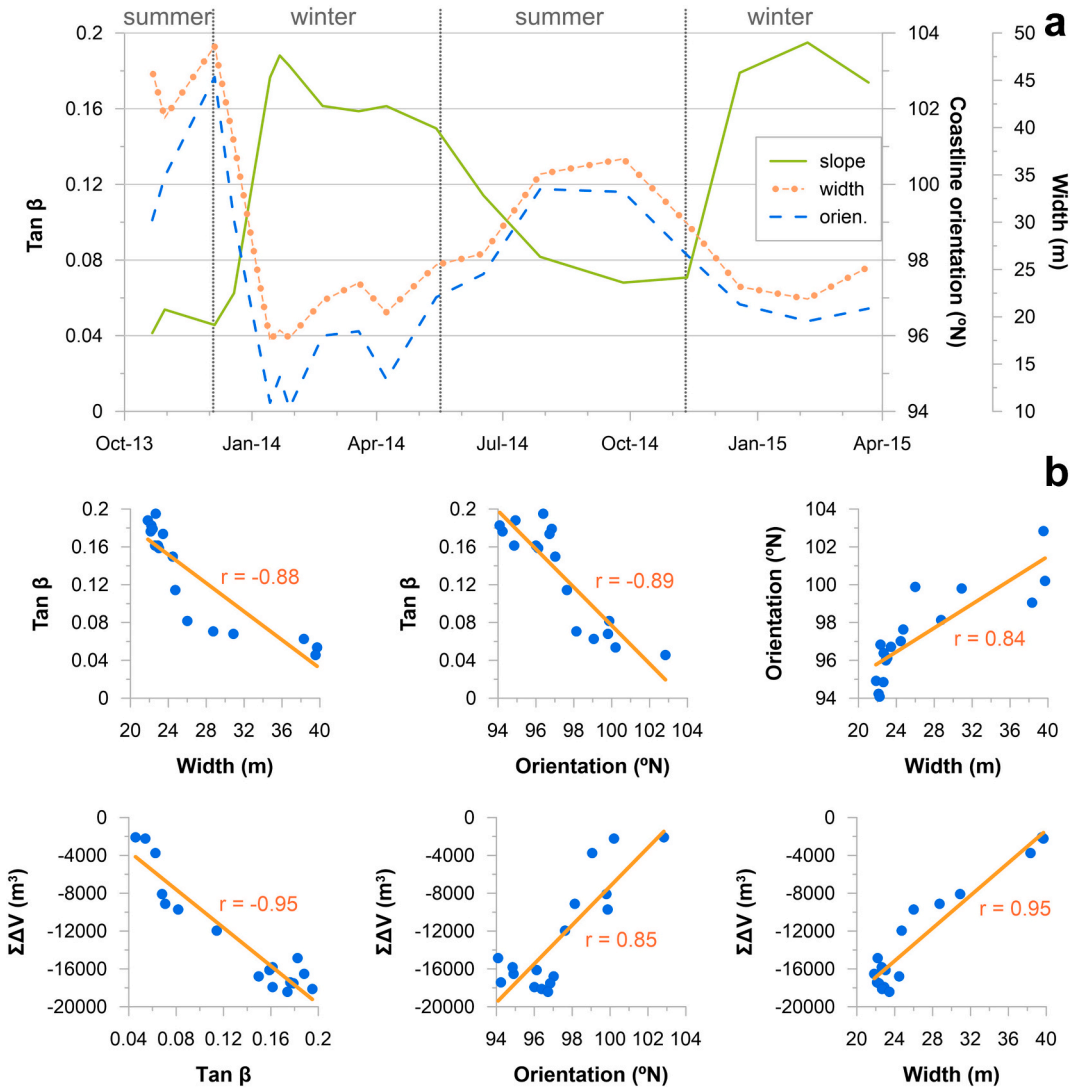

Fig. 10. a) Evolution of morphological variables: slope (tanβ), width and coastline orientation (*orientation*) during the study period. b) Correlation between these variables and the sediment volume.

computed under Stockdon's or Poate's equations shows better correlations coefficients when using offshore wave data than those from the inshore node.

Both the Iribarren number and the surf scaling parameter show statistically significant correlations with the morphological response of the beach. Dean's parameter is the morphodynamic variable with the lowest correlation coefficients (Table 2). Morphodynamic parameters are widely used in coastal geomorphological literature, and they relate the morphological and hydrodynamic characteristics of beaches. The good correlations obtained with the Iribarren number and the surf scaling parameter are mainly due to the fact that both parameters include the beach gradient, which presents a good correlation with the hydrodynamic variables. Regarding the weak correlation of Dean's parameter, it relates to sediment fall velocity and therefore to grain size. Composite beaches present a bimodal distribution with completely different grain size due to the presence of sand in the lower beach face and coarse-grain sediments in the upper profile. Hence, it is difficult to apply parameters that include grain size in their definition.

5. Discussion

Some authors have highlighted the importance of the timescale in field studies (e.g. Pontee et al., 2004). In gravel beaches, tides play an essential role in the control of the swash zone processes and beach profile changes, while wave conditions determine the type of morphological response (Ruiz de Alegria-Arzaburu and Masselink, 2010; Wiggins et al., 2019a, 2019b; Wiggins et al., 2020). For example, Bujan et al. (2019) found that steep beaches could change depending on clast size and wave climate in different timescales. So, whereas sandy and pebble beaches vary on timescales of hours to days, cobble beaches do so on a seasonal or annual basis. The present medium-term study (17 months), conducted in a composite beach with sediments ranging from sand to cobbles, shows a clear seasonal pattern, although the daily timescale is also very important. This shorter timescale can be clearly observed in the strong and quick erosions detected at the beginning of the winter when significant amounts of sand are moved offshore as a consequence of the first energy events of the winter season. Both timescales (days and seasons) are clearly correlated with wave conditions.

San Felipe Beach has a marked seasonal behaviour. Several authors have reported temporal and spatial variations in mixed beaches (e.g., McLean and Kirk, 1969; Pontee et al., 2004; Miller et al., 2011; Atkinson and Esteves, 2018), although there are only a few studies where these changes are associated with seasonality (e.g., Allan et al., 2006; Curtiss et al., 2009). One of the factors that clearly determines the seasonal morphological response of San Felipe Beach is the accumulation and erosion of sand, which mostly takes place during the summer in the mid

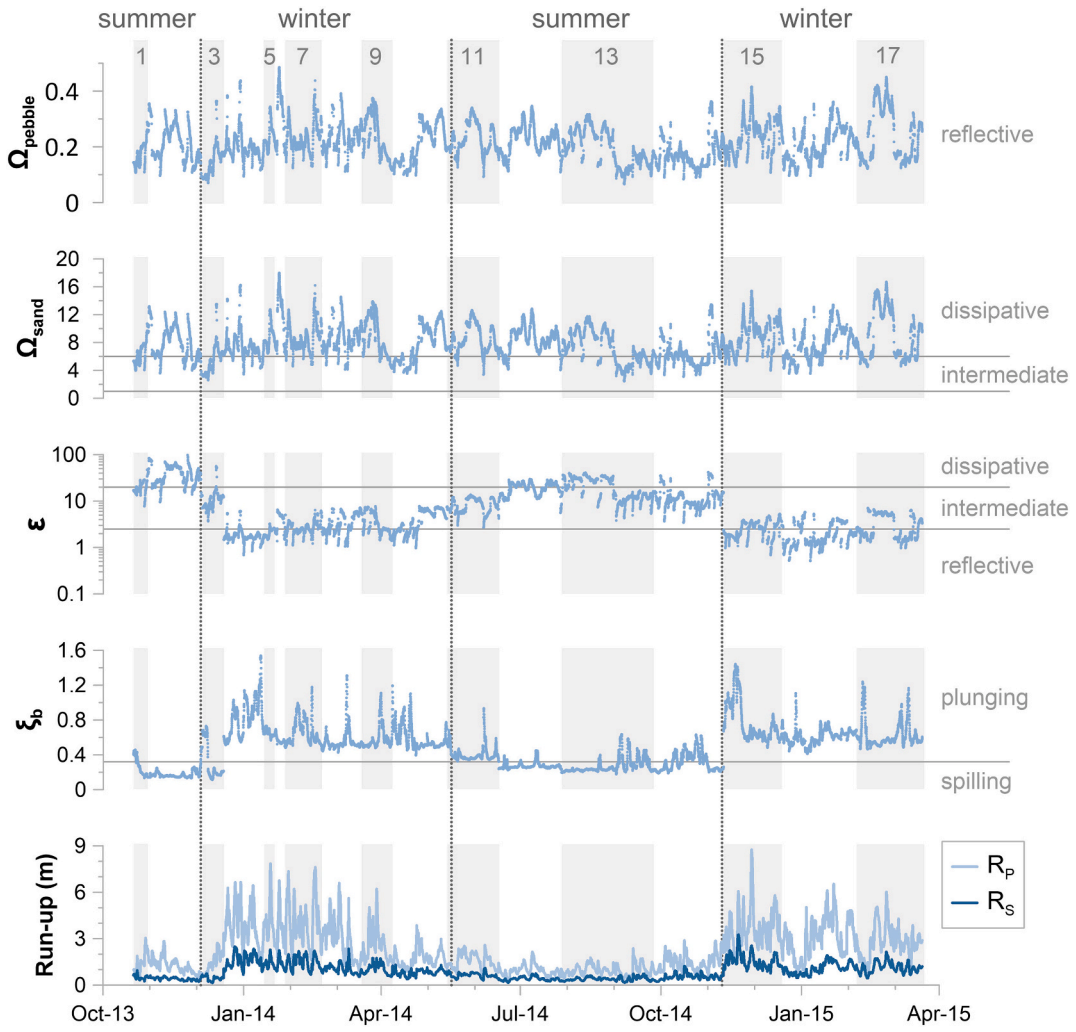

Fig. 11. Temporal evolution of the morphodynamic parameters during the study period in the central offshore node (green triangle in Fig. 1c).

and lower foreshore. This fact determines the strong change in the beach face slope and, subsequently, the morphodynamic behaviour of the beach which, according to the values of the surf scaling parameter (ε), ranges from reflective in winter to dissipative in summer (Fig. 11).

This study shows that the morphodynamic pattern of the beach switches from reflective to dissipative depending on the seasonal inputs/outputs of sand in the foreshore and the redistribution of gravels in the upper profile. Mason and Coates (2001) also report seasonal variations in the sand content of mixed beaches, though they state that it is unlikely that these changes could significantly affect the morphodynamic response of the beach. They base their conclusion on the influence of the proportion of sand in the hydraulic conductivity, which in turn determines the foreshore gradient. This is valid for mixed sand and gravel beaches where both types of sediment coexist across the entire beach profile but is not applicable to composite beaches where the proportion of sand in the upper foreshore is negligible as well as the amount of gravel in the lower foreshore.

Another important factor is the wave climate defined by Pontee et al. (2004) as one of the main factors in the profile variability of mixed beaches. In addition, Curtiss et al. (2009) found that morphologic changes depend on seasonal wave climate variations. The correlation analysis performed between significant wave height and volumetric changes shows a negative relationship: erosion with larger waves and accretion during low energy periods. However, the detailed analysis of the upper and lower part of the profile shows that an onshore movement of coarse-grain sediments takes place with high-energy events, while the fine fraction of sediment is transported offshore.

This onshore transport is common on gravel beaches and leads to the formation of the berm (Buscombe and Masselink, 2006; Horn and Li, 2006; Pedrozo-Acuña et al., 2006; Bertoni and Sarti, 2011), whose position depends on the tidal regime (Orford and Anthony, 2013). Jennings and Shulmeister (2002) determined that the number and height of berms and storm berms shows certain variability, though no clear pattern could be established. According to Carter and Orford (1993), the run-up is the main process responsible for the onshore transport of gravel. This coincides with the results obtained in this study, since run-up is one of the parameters that best correlate with the morphological variables (Table 2). Conversely, some studies have reported that run-up expressions are not accurate predictors in mixed sand and gravel beaches due to the high temporal and spatial variability in the sand/gravel ratio of these systems (López-Ruiz et al., 2020).

The differences detected between the two run-up equations (Eqs. (4) and (5)) used in this study are related to beach slope and therefore, the dissipative/reflective character of the beach. Although Stockdon's equation was provided for more reflective beaches, no data from gravel beaches were included in its development (Poate et al., 2016). Poate's equation arises from the need to include reflective beaches in the existent wave run-up equations, since Masselink et al. (2016) suggest that wave run-up obtained with Stockdon's equation does not present a good fit for gravel beaches of the UK under energetic conditions, since it significantly underestimates the run-up values. However, San Felipe Beach has a great seasonality and while in summer it behaves as a

Table 2
Statistically significant (p-value < 0.01) correlation coefficients (r) of hydrodynamic variables of the central inshore node with respect to the morphological variables. Correlation between morphological and morphodynamic parameters correspond to values of the central offshore node, except for the run-up which was computed both from offshore and inshore node values (subscript off and in respectively). Empty cells and non-listed variables (T_p, wave direction, wave stepness, etc.) correspond to non-statistically significant correlations (p-value > 0.01). Gray values indicate directly related variables.

		Morphological variables					
			up	low	β	width	orientation
Hydrodynamic variables	$\overline{H_s}$	-0.62	0.79	-0.69	0.77		-0.71
	$\overline{H_b}$		0.81	-0.65	0.74		-0.70
	$\overline{E}$		0.77	-0.66	0.74		-0.70
	$\overline{P}$		0.76	-0.61	0.68		-0.65
	E_{cum}		0.81	-0.63	0.68		
	P_{cum}		0.79		0.64		
Morphodynamic variables	$\overline{R_{S_{off}}}$	-0.82	0.77	-0.87	0.90	-0.75	-0.84
	$\overline{R_{P_{off}}}$	-0.76	0.80	-0.82	0.87	-0.69	-0.82
	$\overline{R_{S_{in}}}$	-0.73	0.79	-0.78	0.83	-0.64	-0.78
	$\overline{R_{P_{in}}}$	-0.74	0.80	-0.79	0.85	-0.65	-0.79
	$\overline{\xi_b}$	-0.91	0.69	-0.94	0.93	-0.81	-0.87
	$\overline{\varepsilon}$	0.86		0.86	-0.85	0.81	0.91
	$\overline{\Omega}$				0.64	-0.65	

dissipative beach, in winter it is reflective. Therefore, correlation coefficients with Poate's equation are slightly weaker than those obtained with Stockton's equation. On the other hand, since the upper part of the beach profile has a completely reflective character throughout the year, correlation coefficients fit better with Poate's equation in intermediate and shallow waters. As with the hydrodynamic variables, both the volumetric changes of the upper part and the beach face slope have positive correlations with the run-up. In other words, the higher the run-up the greater the slope and the accumulation of sediments in the upper part (Table 2).

The approach followed in this study to define the limit between the upper and lower parts of the beach has not been used before. The most used division criterion in morphodynamic processes considers the vertical elevation and therefore tanβ derives from MLWS and the storm berm height. However, in composite beaches it is more adequate using the sediment budget to establish the limit, since the resulting zones implicitly incorporates the sediment grain-size characteristics; cobbles and pebbles that are much steadier through the year in the upper profile and the lower part where the sediment changes depending on the season (Figs. 2 and 9).

Regarding the sedimentary balance encompassing the entire study period, the upper part of the beach can be considered in equilibrium whereas the net volume of the lower area is negative, resulting in an overall deficit of sediment over the course of the study period (Fig. 8). The significant erosion that was found can be attributed to different factors. Firstly, the length of the study period (17 months) covers two whole winters and only one whole summer. If the following summer had been monitored, the volumetric difference between the initial and final situation would probably have been smaller. The second reason is directly related to the unusual wave heights recorded during the study period. The two winters monitored during this study were the second and third most energetic ones in the last 28 years (Fig. 4). More specifically, the 2013/14 winter has been described by different authors as the most energetic season on the Atlantic coast of Europe in several decades (Castelle et al., 2015; Masselink et al., 2016; Flor-Blanco et al., 2021).

The Iribarren number led to the identification of two types of breaking waves that follow a strong seasonal variability for the particular case of San Felipe Beach: spilling and plunging (Fig. 11). Plunging breakers prevail in winter while summer is characterized by spilling breakers. There is a clear relationship between this morphodynamic parameter and all the morphological variables analysed, but particularly with respect to volumetric changes in the lower beach face, and the foreshore gradient (Table 2). Pedrozo-Acuña et al. (2008) found that the wave impact of a plunging breaker is an important process in the morphological response of gravel beaches. In addition, Aagaard and Hughes (2010) concluded that plunging breakers generate strong vertical velocities that cause the suspension of bed sediment whereas under spilling breakers this effect is reduced. Hence, the sand erodes from the foreshore when the breaker is plunging type. This material will be gradually deposited on the beach when the breakers change again to spilling type the following summer.

Many hypotheses have been developed regarding beach cusp formation, although there are two models that are the most widely accepted: standing edge waves and the self-organisation model (Coco, 2017). There are still certain gaps in our understanding of cusps, such as cusps evolution timescales, the role played by grain size sorting or whether they are structures associated with erosive or accretion processes (Guest and Hay, 2019). Several authors have described these structures on steep beaches due to their reflective behaviour (e.g., Buscombe and Masselink, 2006; Curoy, 2012; López-Ruiz et al., 2020). The cusps develop along the foreshore by swash flows and normally have a strong difference in sediment grain size, with the horns formed by coarse-grain sediments, while the bays contain finer materials (Buscombe and Masselink, 2006). One of the morphological structures identified in the DEMs is the presence of cusps during winter, since in summer with the sand entrance, San Felipe Beach turns into a dissipative beach, and cusps are only found in reflective and intermediate beaches (Wright and Short, 1984). In both edge wave and self-organisation theories wave period is a variable of the equations to calculate the cusp spacing (Masselink et al., 2004), which is also called cusps wavelength and is defined as the distance between two consecutive horns. According to López-Ruiz et al. (2020) the wavelength of horns is positively correlated with the wave period. In our case this relationship is difficult to evaluate, since cusps are normally present during the winter, but never during summer when sand accumulates on the foreshore.

Regarding the rotation of the coastline, few studies have described the processes behind this phenomenon on gravel and mixed beaches (Ruiz de Alegria-Arzaburu and Masselink, 2010; Dolphin et al., 2011; Wiggins et al., 2019a, 2019b). Dolphin et al. (2011) identified a seasonal pattern in the rotation of a beach situated between two headlands. The key features were a bi-directional wave climate with sufficiently persistent episodes of each wave direction to allow longshore sediment transport to drive sediment from one end to the other. In San Felipe seasonal patterns were identified in wave height and wave period. In summer, smaller and shorter waves (Fig. 5) favour the onshore transport of sand toward the beach. Sand accumulates all along the shoreline, but the accumulation is more intense in the western part of the beach where the lava flow is located. This sharp beach limit contributes to trap the sediments, while there is no equivalent boundary at the eastern side (see Fig. 1d). The sandy deposit is eroded at the beginning of the winter, when higher and larger waves take place. Coastal retreat is more intense at the western part of the beach due to the larger amount of sand. Although beach rotation at San Felipe is related to the different boundary limits at the two ends of the beach, the results of this study show a negative correlation between the direction of the coastline and some of the wave climate parameters (Table 2). This coincides with the

results of other studies which determine the strong influence of seasonal changes of wave climate on beach rotation (e.g., Ruiz de Alegria-Arzaburu and Masselink, 2010; Medellín and Torres-Freyermuth, 2019; Wiggins et al., 2020).

Two main beach states can be identified on San Felipe Beach corresponding to the summer and winter situations. In summer, low-energy wave conditions prevail and sand from the nearshore is transported onshore until it covers the lower and middle foreshore. This cross-shore transport produces several morphological changes: the beach width increases, the beach face slope considerably decreases and the shoreline rotates to the WNE-ESE direction. In summer the percentage of NNE waves increases significantly generating a westward alongshore transport that causes an accumulation of sand in the west due to the presence of the lava flow, which acts as an obstacle for the longshore sediment transport. Waves breaking tends to be the spilling type and the beach is mostly dissipative. In the upper foreshore run-up decreases, but it is still able to build a new berm from the pebbles and cobbles in the area. This berm is located in a lower elevation and closer to the shoreline than the storm berm. The storm berm, generated during the previous high-energy wave conditions, becomes partly dismantled due to the fall of pebbles from the berm crest, a process that is partially induced by beach users on their way to and from the coastline. Nevertheless, this storm berm is clearly recognizable, though both its length and gradient become reduced (Fig. 12).

When the first high-energy event takes place, the sand erodes and is transported offshore, with the beach turning to its winter state. This erosion generates a coastal retreat which is more intense at the western part of the beach, and therefore the shoreline not only migrates onshore but also rotates to a W-E direction. The whole beach becomes covered by large sediments, mostly pebbles and cobbles, except for some sandy patches in the nearshore always below the MLWS. The profile is characterized by a steep slope with cusps along the beach face and a storm berm. The high gradient determines that the beach follows a reflective pattern. The high and long waves are plunging in type and the run-up reaches much higher positions, generating an onshore transport of pebbles. As a result, a storm berm becomes fully developed (Fig. 12).

Following Jennings and Shulmeister (2002), a classification for composite beaches is suggested (Table 3). Although seasonal changes have also been described for other composite beaches (Allan et al., 2006), the seasonal variability described here has not been previously considered in mixed beach classifications. Jennings and Shulmeister (2002) identified daily variations on composite beaches, associated to their tidal-dependent morphodynamic behaviour: a reflective regime should dominate at high tide while a dissipative regime would prevail at low tide. However, these variations have no relation to wave climate or to seasonal variability.

Table 3
Newly proposed classification of gravel beaches based on Jennings and Shulmeister (2002) and the results obtained in this study.

Jennings & Shulmeister (2002) Based on beach gradient and sediment size		Present study Based on wave climate seasonal variability and associated morphological changes	
Pure Gravel		Pure Gravel	
Mixed Sand and Gravel		Mixed Sand and Gravel	
Composite Gravel		Seasonal Composite	
		Pure Gravel (winter)	Composite Gravel (summer)

Jennings and Shulmeister (2002) used field data measured on forty-two gravel beaches from around the coastline of South Island, New Zealand, to define three different types of gravel beaches: pure gravel (PG) beaches, mixed sand and gravel (MSG) beaches and composite gravel (CG) beaches. The beaches they analysed covered a wide range of beach gradient, morphologies and grain size, but these measurements were taken only once at each beach. This study provides the temporal scale using a detailed analysis of the changes that occurred over the course of 17 months on a single mixed beach.

The proposed modification derives from seasonal wave climate variations, which in turn involve seasonal morphological changes on composite beaches. These seasonal changes determine the existence of two different beach states associated to summer and winter situations. The winter state is very similar to the description of PG beaches following the Jennings and Shulmeister (2002) classification, and can be summarised as a steep gravel beaches where cups are normally present

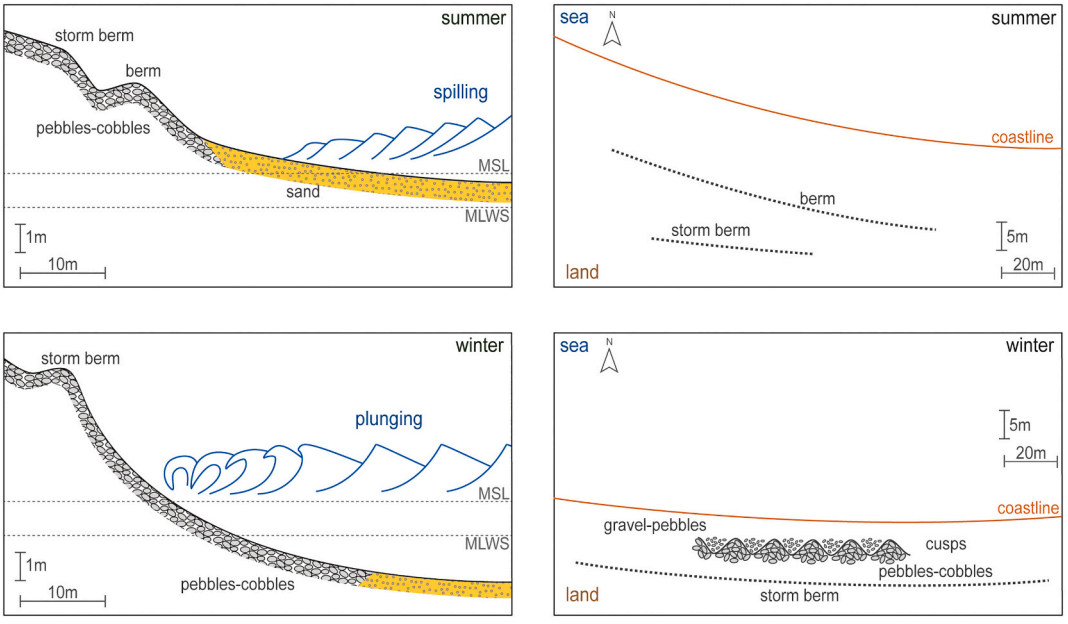

Fig. 12. Schematic representation in cross-section (left) and plain view (right) of the two seasonal states identified at San Felipe Beach. MSL: mean sea level in Las Palmas; MLWS: mean low water spring.

in the beach face and where built up accretion has been observed in the storm berm as a consequence of high-energy events. The summer state follows what Jennings and Shulmeister (2002) classify as CG beaches, with the main characteristic being a two-part profile. The seaward part shows a gentle slope and is sand dominated, while the landward portion is much steeper and coarse-grain sediments dominate (Table 3).

Although MSG and composite beaches have sediments within the same grain size range, their morphological response to wave climate is completely different due to the different sorting of the sediments. For this reason, a research line should be followed to monitor more composite beaches from different environments to confirm if the seasonal pattern described in this paper could be replicated elsewhere.

6. Conclusions

This study presents a detailed space-time analysis of the morphological changes of a composite beach that took place during a period of 17 months. Statistically significant correlations were obtained between several measured morphological variables, morphodynamic parameters and wave forcing conditions. Hence, results have revealed that:

- The method followed to limit the upper and the lower parts of the beach, based on the sediment budget equal to zero when comparing summer and winter DEMs, has shown to be perfectly valid to differentiate two parts of the beach with different morphologies and morphodynamic behaviours.
- San Felipe Beach is a composite beach that follows a marked seasonal behaviour. The seasonal variability that was found in San Felipe Beach enabled the definition of a clear pattern in the seasonal beach characteristics. This pattern differentiates between two different beach states which correspond to the prevailing summer and winter situations.
- The summer state is dominated by small and short spilling waves that favour the onshore transport of sand. The upper profile is steeper and is covered by pebbles and cobbles whereas the lower profile is dominated by sand and gentle gradients.
- The winter state is characterized by high energy wave conditions. Sand is transported offshore, the beach face slope increases and cusps are formed. The run-up reaches higher elevations and moves pebbles upwards, contributing to the creation of a larger storm berm.
- There is an opposite behaviour between the upper and the lower part of the beach. The positive correlation of H_s, H_b, E and P with the volumetric changes in the upper beach face should also be noted, confirming that the higher the wave energy the larger the volume of pebbles in the storm berm and the lower the volume of sand in the foreshore.
- The run-up obtained using Stockdon's equation with offshore wave data and the Iribarren number present very good correlation values with all morphological variables, which confirms their validity to describe morphological changes on composite beaches.
- Results demonstrate that San Felipe Beach does not behave as a composite beach throughout the year. Therefore, a modification of the existing gravel beaches classification is proposed to account for the seasonal morphodynamic changes in this type of beach. The addition of a new seasonal composite beach type allows to differentiate between pure gravel (winter) and composite gravel (summer) behaviours.

Declaration of competing interest

The authors declare that they have no known competing financial interests or personal relationships that could have appeared to influence the work reported in this paper.

Acknowledgements

The authors would like to express their gratitude to all their colleagues who collaborated in the fieldwork and colleagues from the topography department for providing the total station. They are also grateful to three anonymous reviewers and the journal editor for their valuable comments that have greatly helped to improve this manuscript.

References

Aagaard, T., Hughes, M.G., 2010. Breaker turbulence and sediment suspension in the surf zone. Mar. Geol. 271 (3–4), 250–259. https://doi.org/10.1016/J.MARGEO.2010.02.019.

Allan, J.C., Hart, R., Tranquili, J.V., 2006. The use of Passive Integrated Transponder (PIT) tags to trace cobble transport in a mixed sand-and-gravel beach on the high-energy Oregon coast, USA. Mar. Geol. 232 (1–2), 63–86. https://doi.org/10.1016/j.margeo.2006.07.005.

Alonso, I., Casamayor, M., Sánchez García, M.J., Montoya-Montes, I., 2019. Classification and characteristics of beaches at Tenerife and Gran Canaria Islands. In: Morales, J.A. (Ed.), The Spanish Coastal Systems: Dynamic Processes, Sediments and Management. Springer International Publishing, pp. 361–383. https://doi.org/10.1007/978-3-319-93169-2_16.

Aragonés, L., López, I., Villacampa, Y., Serra, J.C., Saval, J.M., 2015. New Methodology for the Classification of Gravel Beaches: Adjusted on Alicante (Spain). J. Coast. Res. 314, 1023–1034. https://doi.org/10.2112/JCOASTRES-D-14-00140.1.

Atkinson, J., Esteves, L.S., 2018. Alongshore variability in the response of a mixed sand and gravel beach to bimodal wave direction. Geosciences (Switzerland) 8 (12). https://doi.org/10.3390/geosciences8120488.

Bascom, W.N., 1951. The relationship between sand size and beach-face slope. EOS Trans. Am. Geophys. Union 32 (6), 866–874. https://doi.org/10.1029/TR032i006p00866.

Battjes, J.A., 1974. Surf similarity. Coast. Eng. Proc. 1 (14), 466–480. https://doi.org/10.9753/icce.v14.26.

Bellido Mulas, F., Pineda Velasco, A., 2008. Mapa Geológico Digital continuo E. 1: 25.000, Zona Canarias - Gran Canaria (Zona-2912). GEODE (online). https://info.igme.es/cartografiadigital/geologica/geodezona.aspx?Id=Z2912.

Bertoni, D., Sarti, G., 2011. On the profile evolution of three artificial pebble beaches at Marina di Pisa, Italy. Geomorphology 130 (3–4), 244–254. https://doi.org/10.1016/j.geomorph.2011.04.002.

Bertoni, D., Sarti, G., Benelli, G., Pozzebon, A., Raguseo, G., 2010. Radio Frequency Identification (RFID) technology applied to the definition of underwater and subaerial coarse sediment movement. Sediment. Geol. 228 (3–4), 140–150. https://doi.org/10.1016/j.sedgeo.2010.04.007.

Bluck, B.J., 1967. Sedimentation of beach gravels; examples from South Wales. J. Sediment. Res. 37 (1), 128–156. https://doi.org/10.1306/74D71672-2B21-11D7-8648000102C1865D.

Booij, N., Ris, R.C., Holthuijsen, L.H., 1999. A third-generation wave model for coastal regions: 1. Model description and validation. Journal of Geophysical Research: Oceans 104 (C4), 7649–7666. https://doi.org/10.1029/98JC02622.

Bramato, S., Ortega-Sánchez, M., Mans, C., Losada, M.A., 2012. Natural recovery of a mixed sand and gravel beach after a sequence of a short duration storm and moderate sea states. J. Coast. Res. 28 (1), 89–101. https://doi.org/10.2112/JCOASTRES-D-10-00019.1.

Bujan, N., Cox, R., Masselink, G., 2019. From fine sand to boulders: Examining the relationship between beach-face slope and sediment size. Mar. Geol. 417, 106012 https://doi.org/10.1016/j.margeo.2019.106012.

Buscombe, D., Masselink, G., 2006. Concepts in gravel beach dynamics. Earth Sci. Rev. 79 (1–2), 33–52. https://doi.org/10.1016/j.earscirev.2006.06.003.

Carter, R.W.G., Orford, J.D., 1993. The morphodynamics of coarse clastic beaches and barriers: a short- and long-term perspective. J. Coast. Res. 158–179. http://www.jstor.org/stable/25735728.

Casamayor, M., Alonso, I., Cabrera, J., Rodríguez, S., Sánchez-García, M., 2015. Long term recovery rates obtained using RFID technology at a mixed beach. Geol. Acta 13 (2), 85–96. https://doi.org/10.1344/GeologicaActa2015.13.2.1.

Castelle, B., Marieu, V., Bujan, S., Splinter, K.D., Robinet, A., Sénéchal, N., Ferreira, S., 2015. Impact of the winter 2013–2014 series of severe Western Europe storms on a double-barred sandy coast: beach and dune erosion and megacusp embayments. Geomorphology 238, 135–148. https://doi.org/10.1016/J.GEOMORPH.2015.03.006.

Ciavola, P., Castiglione, E., 2009. Sediment dynamics of mixed sand and gravel beaches at short time-scales. J. Coast. Res. 1751–1755. http://www.jstor.org/stable/25738090.

Coco, G., 2017. Beach Cusps. Atlas of Bedforms in the Western Mediterranean. Springer International Publishing, pp. 55–57. https://doi.org/10.1007/978-3-319-33940-5_10.

Copernicus Marine Service, 2020. Product user manual for Atlantic-Iberian Biscay Irish-wave Reanalysis: IBI_MULTIYEAR_WAV_005_006. https://catalogue.marine.copernicus.eu/documents/PUM/CMEMS-IBI-PUM-005-006.pdf.

Curoy, J., 2012. Morphological and longshore sediment transport processes on mixed beaches. University of Sussex.

Curtiss, G.M., Osborne, P.D., Horner-Devine, A.R., 2009. Seasonal patterns of coarse sediment transport on a mixed sand and gravel beach due to vessel wakes, wind

waves, and tidal currents. Mar. Geol. 259 (1–4), 73–85. https://doi.org/10.1016/j.margeo.2008.12.009.
Dean, R.G., 1973. Heuristic models of sand transport in the surf zone. In: Proceedings of the Conference on Engineering Dynamics in the Surf Zone, pp. 208–214.
Dickson, M.E., Kench, P.S., Kantor, M.S., 2011. Longshore transport of cobbles on a mixed sand and gravel beach, southern Hawke Bay, New Zealand. Marine Geology 287 (1–4), 31–42. https://doi.org/10.1016/j.margeo.2011.06.009.
Dolphin, T.J., Vincent, C.E., Wihsgott, J., Belhache, M., Bryan, K.R., 2011. Seasonal rotation of a mixed sand-gravel beach (Proceedings of the 11th International Coastal Symposium). J. Coast. Res. 64 (SPEC. ISSUE 64), 65–69. https://hdl.handle.net/10289/5741.
Flor-Blanco, G., Alcántara-Carrió, J., Jackson, D.W.T., Flor, G., Flores-Soriano, C., 2021. Coastal erosion in NW Spain: recent patterns under extreme storm wave events. Geomorphology 387, 107767. https://doi.org/10.1016/J.GEOMORPH.2021.107767.
Gonçalves, M., Martinho, P., Guedes Soares, C., 2014. Assessment of wave energy in the Canary Islands. Renew. Energy 68, 774–784. https://doi.org/10.1016/j.renene.2014.03.017.
Grottoli, E., Bertoni, D., Pozzebon, A., Ciavola, P., 2019. Influence of particle shape on pebble transport in a mixed sand and gravel beach during low energy conditions: implications for nourishment projects. Ocean Coast. Manag. 169, 171–181. https://doi.org/10.1016/j.ocecoaman.2018.12.014.
Guest, T.B., Hay, A.E., 2019. Timescales of beach cusp evolution on a steep, megatidal, mixed sand-gravel beach. Mar. Geol. 416 (3) https://doi.org/10.1016/j.margeo.2019.105984.
Herbich, J.B., 2000. Handbook of Coastal Engineering. McGraw-Hill.
Holland, K.T., Elmore, P.A., 2008. A review of heterogeneous sediments in coastal environments. Earth Sci. Rev. 89 (3–4), 116–134. https://doi.org/10.1016/j.earscirev.2008.03.003.
Horn, D., Li, L., 2006. Measurement and modelling of gravel beach groundwater response to wave run-up: effects on beach profile changes. J. Coast. Res. 22 (5), 1241–1249. https://doi.org/10.2112/06A-0006.1.
Horn, D.P., Walton, S.M., 2007. Spatial and temporal variations of sediment size on a mixed sand and gravel beach. Sediment. Geol. 202 (3), 509–528. https://doi.org/10.1016/j.sedgeo.2007.03.023.
Ivamy, M.C., Kench, P.S., 2006. Hydrodynamics and morphological adjustment of a mixed sand and gravel beach, Torere, Bay of Plenty New Zealand. Mar. Geol. 228 (1–4), 137–152. https://doi.org/10.1016/j.margeo.2006.01.002.
Jennings, R., Shulmeister, J., 2002. A field based classification scheme for gravel beaches. Mar. Geol. 186 (3–4), 211–228. https://doi.org/10.1016/S0025-3227(02)00314-6.
Kirk, R.M., 1970. Swash zone processes: An examination of water motion and the relations between water motion and foreshore response on some mixed sand and shingle beaches, Kaikoura, New Zealand. In: Geography. University of Canterbury. https://doi.org/10.26021/5620.
Komar, P.D., Gaughan, M.K., 1972. Airy wave theory and breaker height prediction. Coast. Eng. Proc. 1 (13 SE-Conference Proceedings) https://doi.org/10.9753/icce.v13.20.
Komen, G.J., Hasselmann, S., Hasselmann, K., 1984. On the existence of a fully developed wind-sea spectrum. J. Phys. Oceanogr. 14 (8, Aug. 1), 1271–1285. https://doi.org/10.1175/1520-0485(1984)014<1271:oteoaf>2.0.co;2.
López-Ruiz, A., Ortega-Sánchez, M., Losada, M.Á., 2020. Mixed sand and gravel beaches. In: Sandy Beach Morphodynamics. Elsevier, pp. 317–341. https://doi.org/10.1016/b978-0-08-102927-5.00014-x.
de San, López, Román-Blanco, B., Coates, T.T., Holmes, P., Chadwick, A.J., Bradbury, A., Baldock, T.E., Pedrozo-Acuña, A., Lawrence, J., Grüne, J., 2006. Large scale experiments on gravel and mixed beaches: experimental procedure, data documentation and initial results. Coast. Eng. 53 (4), 349–362. https://doi.org/10.1016/j.coastaleng.2005.10.021.
Maestro-González, A., Medialdea-Cela, T., Llave-Barranco, E., Somoza-Losada, L., León-Buendía, R., 2005. El margen continental de las Islas Canarias. In: Serrano, A. Martín (Ed.), Mapa Geomorfológico de España y del margen continental a escala 1:1000000. IGME, pp. 229–232.
Mangas Viñuela, J., 2020. Génesis y evolución geológica de Gran Canaria: un buen ejemplo de la geodiversidad de una isla volcánica intraplaca oceánica. In: Carrillo, J. M. Afonso (Ed.), Actas de la XV Semana Científica Telesforo Bravo: Gran Canaria. Las huellas del tiempo. Instituto de Estudios Hispánicos de Canarias, p. 61. https://accedacris.ulpgc.es/handle/10553/75225#.YAq7YZcnFyk.mendeley.
Mason, T., Coates, T.T., 2001. Sediment transport processes on mixed beaches: a review for shoreline management. J. Coast. Res. 17 (3), 645–657. http://www.jstor.org/stable/4300216.
Masselink, G., Russell, P., Coco, G., Huntley, D., 2004. Test of edge wave forcing during formation of rhythmic beach morphology. J. Geophys. Res. Oceans 109 (C6). https://doi.org/10.1029/2004JC002339.
Masselink, G., Scott, T., Poate, T., Russell, P., Davidson, M., Conley, D., 2016. The extreme 2013/2014 winter storms: hydrodynamic forcing and coastal response along the southwest coast of England. Earth Surf. Process. Landf. 41 (3), 378–391. https://doi.org/10.1002/esp.3836.
McLean, R.F., Kirk, R.M., 1969. Relationships between grain size, size-sorting, and foreshore slope on mixed sand - shingle beaches. N. Z. J. Geol. Geophys. 12 (1), 138–155. https://doi.org/10.1080/00288306.1969.10420231.
Medellín, G., Torres-Freyermuth, A., 2019. Morphodynamics along a micro-tidal sea breeze dominated beach in the vicinity of coastal structures. Mar. Geol. 417, 106013 https://doi.org/10.1016/j.margeo.2019.106013.
Miller, I.M., Warrick, J.A., Morgan, C., 2011. Observations of coarse sediment movements on the mixed beach of the Elwha Delta, Washington. Mar. Geol. 282 (3–4), 201–214. https://doi.org/10.1016/j.margeo.2011.02.012.
Nielsen, P., Hanslow, D.J., 1991. Wave runup distributions on natural beaches. J. Coast. Res. 7 (4), 1139–1152. http://www.jstor.org/stable/4297933.
Orford, J., Anthony, E., 2013. Coastal gravel systems. In: Treatise on Geomorphology, Vol. 10. Academic Press, pp. 245–266. https://doi.org/10.1016/B978-0-12-374739-6.00280-3.
Orford, J.D., 1975. Discrimination of particle zonation on a pebble beach. Sedimentology 22 (3), 441–463. https://doi.org/10.1111/j.1365-3091.1975.tb01640.x.
Osborne, P.D., 2005. Transport of gravel and cobble on a mixed-sediment inner bank shoreline of a large inlet, Grays Harbor, Washington. Mar. Geol. 224 (1–4), 145–156. https://doi.org/10.1016/j.margeo.2005.08.004.
Pedrozo-Acuña, A., Simmonds, D.J., Chadwick, A.J., Silva, R., 2007. A numerical-empirical approach for evaluating morphodynamic processes on gravel and mixed sand-gravel beaches. Mar. Geol. 241 (1–4), 1–18. https://doi.org/10.1016/j.margeo.2007.02.013.
Pedrozo-Acuña, A., Simmonds, D.J., Otta, A.K., Chadwick, A.J., 2006. On the cross-shore profile change of gravel beaches. Coast. Eng. 53 (4), 335–347. https://doi.org/10.1016/j.coastaleng.2005.10.019.
Pedrozo-Acuña, A., Simmonds, D.J., Reeve, D.E., 2008. Wave-impact characteristics of plunging breakers acting on gravel beaches. Mar. Geol. 253 (1–2), 26–35. https://doi.org/10.1016/j.margeo.2008.04.013.
Pitman, S., Hart, D., Katurji, M., 2019. Beach cusp morphodynamics on a composite beach observed using UAV structure from motion. September 10. In: Australasian Coasts & Ports.
Poate, T.G., McCall, R.T., Masselink, G., 2016. A new parameterisation for runup on gravel beaches. Coast. Eng. 117, 176–190. https://doi.org/10.1016/j.coastaleng.2016.08.003.
Pontee, N.I., Pye, K., Blott, S.J., 2004. Morphodynamic behaviour and sedimentary variation of mixed sand and gravel beaches, Suffolk, UK. J. Coast. Res. 20 (1), 256–276. http://www.jstor.org/stable/4299281.
Powell, K.A., 1990. Predicting Short Term Profile Response for Shingle Beahces.
Puertos del Estado, 2018. Clima medio de oleaje. Nodo SIMAR 4035011. https://bancodatos.puertos.es/BD/informes/medios/MED_1_8_4035011.pdf.
Puertos del Estado, 2019. REDMAR: Resumen de parámetros relacionados con el nivel del mar y la marea que afectan a las condiciones de diseño y explotación portuaria. https://bancodatos.puertos.es/BD/informes/globales/GLOB_2_3_3450.pdf.
Puertos del Estado, 2020. Conjunto de datos SIMAR. https://bancodatos.puertos.es/BD/informes/INT_8.pdf.
Pye, K., 2001. The nature and geomorphology of coastal shingle. In: Packham, J., Randall, R., Barnes, R.S.K., Neal, A. (Eds.), Ecology and Geomorphology of Coastal Shingle. Smith Settle, pp. 2–22.
Roberts, T.M., Wang, P., Puleo, J.A., 2013. Storm-driven cyclic beach morphodynamics of a mixed sand and gravel beach along the Mid-Atlantic Coast, USA. Mar. Geol. 346, 403–421. https://doi.org/10.1016/j.margeo.2013.08.001.
Ruiz de Alegria-Arzaburu, A., Masselink, G., 2010. Storm response and beach rotation on a gravel beach, Slapton Sands, U.K. Mar. Geol. 278 (1–4), 77–99. https://doi.org/10.1016/j.margeo.2010.09.004.
Sánchez, M.J., Quartao, R., Alonso, I., Montoya-Montes, I., Casamayor, M., Rodríguez, S., 2017. Rasgos morfológicos del margen insular de la isla de Gran Canaria. In: Buades, G. Pons, Lorenzo-Lacruz, J., Pujol, L. Gómez (Eds.), Geotemas. Sociedad Geológica de España, pp. 331–334. https://accedacris.ulpgc.es/handle/10553/57377#.YArTeUuP_mo.mendeley.
Schmincke, H.-U., 1982. Volcanic and chemical evolution of the Canary Islands. In: von Rad Ulrich, K., Hinz, Michael, S., Eugen, S. (Eds.), Geology of the Northwest African Continental Margin. Springer, Berlin Heidelberg, pp. 273–306.
Soulsby, R., 1997. Dynamics of Marine Sands: A Manual for Practical Applications. Thomas Telford Publishing. https://doi.org/10.1680/doms.25844.
Stockdon, H.F., Holman, R.A., Howd, P.A., Sallenger, A.H., 2006. Empirical parameterization of setup, swash, and runup. Coast. Eng. 53 (7), 573–588. https://doi.org/10.1016/j.coastaleng.2005.12.005.
Stokes, C., Russell, P., Davidson, M., 2016. Sub-tidal and inter-tidal three-dimensionality at a high energy macrotidal beach. J. Coast. Res. 75 (sp1), 472–476. https://doi.org/10.2112/SI75-095.1.
Valiente, N.G., McCarroll, R.J., Masselink, G., Scott, T., Wiggins, M., 2019. Multi-annual embayment sediment dynamics involving headland bypassing and sediment exchange across the depth of closure. Geomorphology 343, 48–64. https://doi.org/10.1016/j.geomorph.2019.06.020.
Van Wellen, E., Chadwick, A.J., Mason, T., 2000. A review and assessment of longshore sediment transport equations for coarse-grained beaches. Coast. Eng. 40 (3), 243–275. https://doi.org/10.1016/S0378-3839(00)00031-4.
Watt, T., Robinson, D.A., Moses, C.A., Dornbusch, U., 2008. Patterns of surface sediment grain size distribution under the influence of varying wave conditions on a mixed sediment beach at Pevensey Bay, Southeast England. Zeitschrift Für Geomorphologie, Suppl. Issues 52 (3), 63–77. https://doi.org/10.1127/0372-8854/2008/0052S3-0063.
Wiggins, M., Scott, T., Masselink, G., McCarroll, R.J., Russell, P., 2020. Predicting beach rotation using multiple atmospheric indices. Mar. Geol. 426, 106207 https://doi.org/10.1016/J.MARGEO.2020.106207.
Wiggins, M., Scott, T., Masselink, G., Russell, P., McCarroll, R.J., 2019a. Coastal embayment rotation: response to extreme events and climate control, using full embayment surveys. Geomorphology 327, 385–403. https://doi.org/10.1016/J.GEOMORPH.2018.11.014.

Wiggins, M., Scott, T., Masselink, G., Russell, P., Valiente, N.G., 2019b. Regionally-coherent embayment rotation: behavioural response to bi-directional waves and atmospheric forcing. J. Mar. Sci. Eng. 7 (4) https://doi.org/10.3390/jmse7040116.
Williams, A.T., Caldwell, N.E., 1988. Particle size and shape in pebble-beach sedimentation. Mar. Geol. 82 (3–4), 199–215. https://doi.org/10.1016/0025-3227(88)90141-7.
Wright, L.D., Short, A.D., 1984. Morphodynamic variability of surf zones and beaches: a synthesis. Mar. Geol. 56 (1–4), 93–118. https://doi.org/10.1016/0025-3227(84)90008-2.